



Article

Pharmacomodulation of the Redox-Active Lead Plasmodione: Synthesis of Substituted 2-Benzyl-naphthoquinone Derivatives, Antiplasmodial Activities, and Physicochemical Properties

Armin Presser ^{1,*} , Gregor Blaser ¹, Eva-Maria Pferschy-Wenzig ² , Marcel Kaiser ^{3,4}, Pascal Mäser ^{3,4} and Wolfgang Schuehly ²

¹ Institute of Pharmaceutical Sciences, Pharmaceutical Chemistry, University of Graz, Schubertstrasse 1, 8010 Graz, Austria; gregor.blaser@gmx.at

² Institute of Pharmaceutical Sciences, Pharmacognosy, University of Graz, Beethovenstrasse 8, 8010 Graz, Austria; eva-maria.wenzig@uni-graz.at (E.-M.P.-W.); wolfgang.schuehly@uni-graz.at (W.S.)

³ Swiss Tropical and Public Health Institute, Kreuzstrasse 2, 4123 Allschwil, Switzerland; marcel.kaiser@swisstph.ch or marcel.kaiser@unibas.ch (M.K.); pascal.maeser@swisstph.ch or pascal.maeser@unibas.ch (P.M.)

⁴ Faculty of Philosophy and Natural Sciences, University of Basel, Petersplatz 1, 4003 Basel, Switzerland

* Correspondence: armin.presser@uni-graz.at; Tel.: +43-316-380-5369

Abstract: Malaria remains a major global health problem that has been exacerbated by the impact of the COVID-19 pandemic on health systems. To combat this, the World Health Organization (WHO) has set a target of driving forward research into innovative treatment methods such as new drugs and vaccines. Quinones, particularly 1,4-naphthoquinones, have been identified as promising candidates for the development of antiprotozoal drugs. Herein, we report several methods for the preparation of 2-benzyl-1,4-naphthoquinones. In particular, the silver-catalyzed Kochi–Anderson radical decarboxylation is well suited for the preparation of these compounds. The antiprotozoal activity of all synthesized compounds was evaluated against *Plasmodium falciparum* NF54 and *Trypanosoma brucei rhodesiense* STIB900. Cytotoxicity towards L6 cells was also determined, and the respective selectivity indices (SI) were calculated. The synthesized compounds exhibited good antiplasmodial activity against the *P. falciparum* (NF54) strain, particularly (2-fluoro-5-trifluoromethylbenzyl)-menadione **2e**, which showed strong efficacy and high selectivity (IC₅₀ = 0.006 μM, SI = 7495). In addition, these compounds also displayed favorable physicochemical properties, suggesting that the benzylnaphthoquinone scaffold may be a viable option for new antiplasmodial drugs.

Keywords: antiprotozoal activity; plasmodione; Kochi–Anderson reaction; physicochemical parameters; ligand efficiency indices



Academic Editor: Davide Moi

Received: 31 January 2025

Revised: 24 February 2025

Accepted: 25 February 2025

Published: 27 February 2025

Citation: Presser, A.; Blaser, G.; Pferschy-Wenzig, E.-M.; Kaiser, M.; Mäser, P.; Schuehly, W.

Pharmacomodulation of the Redox-Active Lead Plasmodione: Synthesis of Substituted 2-Benzyl-naphthoquinone Derivatives, Antiplasmodial Activities, and Physicochemical Properties. *Int. J. Mol. Sci.* **2025**, *26*, 2114. <https://doi.org/10.3390/ijms26052114>

Copyright: © 2025 by the authors. Licensee MDPI, Basel, Switzerland. This article is an open access article distributed under the terms and conditions of the Creative Commons Attribution (CC BY) license (<https://creativecommons.org/licenses/by/4.0/>).

1. Introduction

Malaria, one of the world's most malignant diseases, continues to be a major global health problem, especially in tropical and subtropical regions. In 2022, the World Health Organization (WHO) reported 249 million cases of malaria worldwide that caused an estimated 608,000 deaths in 85 countries [1]. This number demonstrates a significant worsening of the malaria situation compared to 2019 as a consequence of the global COVID-19 pandemic, which has resulted in strained health systems and diverted resources. In response to the ongoing challenges, WHO has updated its malaria strategy and its aims at reducing malaria cases and deaths by 90% by 2030 [2]. This ambitious goal may only be

achieved through a renewed commitment to innovative strategies, e.g., effective malaria vaccines [3] and the development of new antimalarial drugs [4].

Quinones have recently regained increasing interest in the field of medicinal chemistry, particularly in the discovery of new drugs for the treatment of neglected tropical parasitic diseases [5–8]. The quinone scaffold is found in a variety of secondary plant metabolites, e.g., lapachol or plumbagin (Figure 1), with a broad spectrum of biological activities [9–13]. Among the various quinone types, the 1,4-naphthoquinone (NQ) scaffold has been identified as a promising pharmacophore for further drug development due to its activity against various apicomplexan parasites, above all, the malaria pathogens of the subgroup *Plasmodium* [13–17].

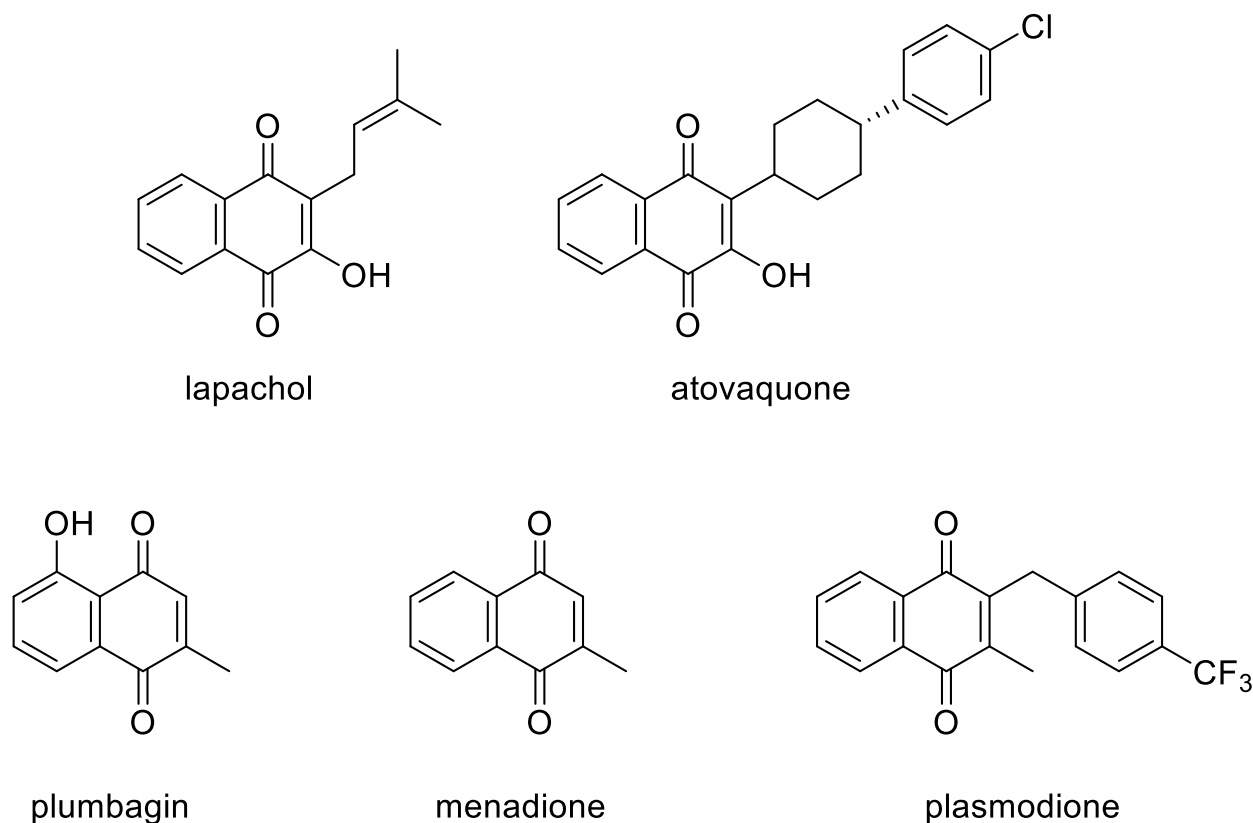


Figure 1. 1,4-Naphthoquinones with remarkable biological activity.

In this context, a redox-active compound called plasmodione (**2b**), a member of the benzylmenadione family with a unique mechanism of action, has shown particularly promising profiles [18–22]. Plasmodione kills parasites as efficiently as the currently most efficient available drug, i.e., artemisinin, besides, it is effective against many drug-resistant parasites and shows a low potential for the development of genetic resistance [21]. Furthermore, despite its chemical similarity to the common antimalarial drug atovaquone, plasmodione does not target the same mitochondrial protein and is therefore effective against atovaquone-resistant strains [23].

In the present study, we synthesized 27 plasmodione-like derivatives with a benzyl-naphthoquinone core to investigate their antimalarial potential in comparison to the original lead plasmodione. To assess the druggability of our synthesized compounds, we also analyzed the safety profile, various physicochemical parameters, and ligand efficiency metrics.

2. Results and Discussion

2.1. Synthetic Chemistry

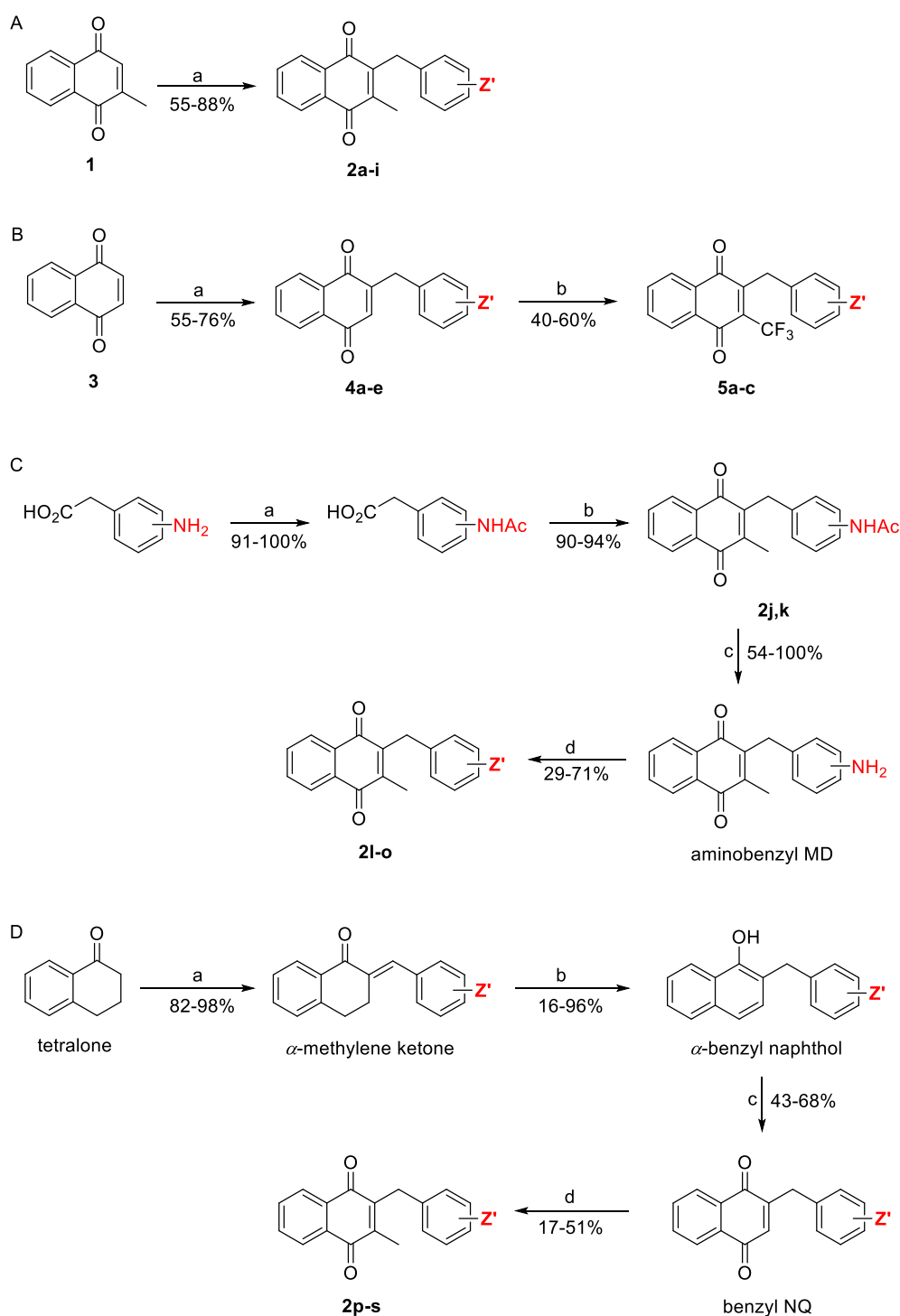
There are several chemical routes to introduce a benzyl moiety into the 1,4-naphthoquinone scaffold [24,25], including a silver-catalyzed decarboxylative cross-coupling of the 1,4-naphthoquinone core with carboxylic acids [20,26], an iron-catalyzed or light-induced radical benzylation of quinones starting from benzyl bromides [27,28], or optionally via a four-step route based on tetralone [26,29].

The silver-catalyzed radical decarboxylation reaction (Kochi–Anderson reaction) [30] provides a powerful tool for fast and easy access to 2-methyl-1,4-naphthoquinone (menadione, **1**) derivatives in only one step. By using this method, we first synthesized a series of menadione (MD) derivatives (**2a–i**) from commercial phenylacetic acids in good to moderate yields (55–88%, Scheme 1, route A). The reaction was compatible with a wide range of substituents, such as halogens, trifluoromethoxy, or nitro groups. For the preparation of benzylated desmethyl derivatives (**4a–e**), the conditions had to be slightly modified to avoid the formation of disubstituted products (Scheme 1, route B).

Trifluoromenadione has also been proposed as a promising core for antimalarial drugs [31]. Therefore, a series of benzylated trifluoromenadiones (**5a–c**) were prepared from the previously obtained naphthoquinones **4a–c** via a direct copper-catalyzed C–H trifluoromethylation [32–34]. Interestingly, the reaction was only successful when a different approach to the published procedure was applied, such as the mandatory addition of bis(pinacolato)diboron (B_2pin_2) and the presence of CuI as a catalyst. Under these optimized conditions (which are described in detail in Section 3), the trifluoromenadiones **5a–c** could be obtained in satisfactory yields.

Urgin and co-workers [35] investigated the antimalarial potential of N-substituted benzylmenadiones and found unexpectedly high antimalarial activity in their N-tert-butoxycarbonyl-protected intermediates. The same authors also report that a Kochi–Anderson benzylation of unprotected amino phenylacetic acids is not successful and leads mainly to degradation of the starting materials. We have taken these observations as an incentive to investigate the antimalarial potential of a few (mainly fluorinated) amidobenzylmenadiones wherein a microwave-assisted N-acetyl-protection strategy was used to achieve this goal (Scheme 1, route C). In this way, the acetamidobenzyl derivatives **2j,k** were obtained excellently and the fluorinated derivatives **2l–o** in good to moderate yields.

Due to the limited choice of commercially available phenylacetic acids, we have taken an alternative 4-step route, starting from commercial tetralone via the corresponding α -methylene ketones and α -benzylnaphthols to the final benzylmenadione derivatives (Scheme 1, route D). In this alternative scenario, the final benzylic chain is already introduced in the first step by coupling with various benzaldehydes [26,29]. However, the tedious synthetic route in combination with the rather poor stability of the methyl radical in the final Kochi–Anderson step has led to overall not impressive yields for the benzylmenadiones **2p–s**. Nevertheless, sufficient material for biological evaluations could be obtained. Overall yields of all synthesized naphthoquinone and menadione derivatives are presented in Table 1.

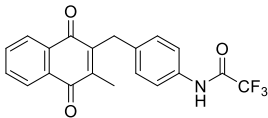
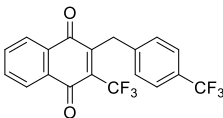
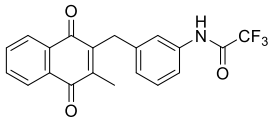
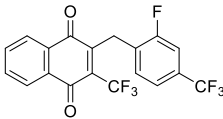
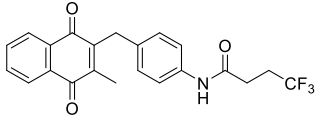


Scheme 1. Synthesis of benzyl-substituted naphthoquinone and menadione derivatives via Kochi–Anderson reaction (**A–C**) or an alternative tetralone route (**D**). Reagents and conditions: (**A**): (a) phenylacetic acid derivative (1.4 equiv.), AgNO₃ (0.35 equiv.), (NH₄)₂S₂O₈ (1.3 equiv.), CH₃CN/H₂O, 85 °C, 1–4 h. (**B**): (a) phenylacetic acid derivative (1.4 equiv.), AgNO₃ (0.1 equiv.), (NH₄)₂S₂O₈ (2 equiv.), CH₃CN/CH₂Cl₂, 80 °C, 1.5–2.5 h; (b). CuI (0.5 equiv.), B₂pin₂ (0.01 equiv.), Togni reagent (2 equiv.), CHCl₃, 85 °C, 20–26 h. (**C**): (a) AcOH, mw, 150 °C, 40 min; (b) acetaminophenylacetic acid (2 equiv.), menadione (1 equiv.), AgNO₃ (0.35 equiv.), (NH₄)₂S₂O₈ (1.3 equiv.), CH₃CN/H₂O, 85 °C, 1.5 h; (c) MeOH/HCl *conc.*, mw, 150 °C, 30 min; (d) carboxylic acid (1 equiv.), DCC (1.2 equiv.), DMF, rt, 3–4 h. (**D**): (a) benzaldehyde derivative (1.1 equiv.), KOH/EtOH, rt, 2.5–4 h; (b) RhCl₃ (0.1 equiv.), EtOH, 85 °C, 24 h; (c) PIDA (2.1 equiv.), CH₃CN/H₂O, −5 °C → rt, 1.5 h; (d) AcOH (5 equiv.), AgNO₃ (0.35 equiv.), (NH₄)₂S₂O₈ (1.3 equiv.), CH₃CN/H₂O, 85 °C, 3 h.

Table 1. Synthesis of benzyl-substituted naphthoquinone and menadione derivatives (overall yields calculated from NQ, MD, and tetralone).

Compd	Structure	Route	Yield (%)	Compd	Structure	Route	Yield (%)
2a		A	88	2o		C	14
2b		A	83	2p		D	17
2c		A	69	2q		D	<5
2d		A	66	2r		D	<5
2e		A	63	2s		D	<5
2f		A	60	4a		B	75
2g		A	66	4b		B	66
2h		A	58	4c		B	58
2i		A	55	4d		B	61
2j		C	94	4e		B	55
2k		C	90	5a		B	45

Table 1. Cont.

Compd	Structure	Route	Yield (%)	Compd	Structure	Route	Yield (%)
2l		C	67	5b		B	38
2m		C	28	5c		B	23
2n		C	66				

2.2. Biological Evaluation

The synthesized benzylmenadione and naphthoquinone derivatives were tested *in vitro* for their antiprotozoal activity against *P. falciparum* (NF54) erythrocytic stages and *T. brucei rhodesiense* (STIB900) bloodstream forms. Cytotoxicity was assessed towards rat L6 skeletal muscle cells to calculate a selectivity index for each parasite ($SI = IC_{50}(L6)/IC_{50}(\text{parasite})$).

According to the recommended hit-to-lead identification criteria [36–38], most of the derivatives showed good to very good antiplasmodial activity against NF54 (Table 2), with the (2-fluoro-5-trifluoromethylbenzyl) menadione **2e** exhibiting the strongest activity ($IC_{50} = 0.006 \mu\text{M}$) along with the highest selectivity ($SI = 7495$). Trypanocidal activity was also observed (strongest with benzyl-NQ **4a**), but generally much lower.

Table 2. In vitro antiparasitic activity, mammalian cell toxicity, and predicted oral toxicity of the synthesized compounds.

Compd	<i>P. falc.</i> ¹ $IC_{50} \mu\text{M}$	SI ²	<i>P. falc.</i> ¹ pIC_{50} ⁵	<i>T. b. rhod.</i> ³ $IC_{50} \mu\text{M}$	SI ²	<i>T. b. rhod.</i> ³ pIC_{50} ⁵	Cyt L6 ⁴ $IC_{50} \mu\text{M}$	Oral Toxicity ⁶ $LD_{50} \text{mg/kg}$
Chl.	0.003	30367	8.52				91.1	
Mel.				0.006	4033	8.22	24.2	
Pod.							0.024	
2a	0.358	126	6.45	62.793	1	4.20	45.023	500
2b	0.048	994	7.31	65.276	1	4.19	48.152	500
2c	0.011	5377	7.94	81.396	1	4.09	61.746	500
2d	0.020	3099	7.70	23.210	3	4.63	62.274	500
2e	0.006	7495	8.24	93.021	0	4.03	43.038	2000
2f	0.037	654	7.43	8.269	3	5.08	24.172	2000
2g	0.111	172	6.96	28.034	1	4.55	19.069	500
2h	0.022	810	7.67	25.543	1	4.59	17.427	500
2i	0.044	1231	7.35	30.353	2	4.52	54.509	500

Table 2. Cont.

Compd	<i>P. falc.</i> ¹ IC ₅₀ µM	SI ²	<i>P. falc.</i> ¹ pIC ₅₀ ⁵	<i>T. b. rhod.</i> ³ IC ₅₀ µM	SI ²	<i>T. b. rhod.</i> ³ pIC ₅₀ ⁵	Cyt L6 ⁴ IC ₅₀ µM	Oral Toxicity ⁶ LD ₅₀ mg/kg
2j	0.695	24	6.16	28.886	1	4.54	16.317	500
2k	0.758	22	6.12	39.457	0	4.40	16.568	1000
2l	0.147	109	6.83	23.384	1	4.63	16.109	1033
2m	0.321	43	6.49	24.265	1	4.62	13.706	948
2n	0.159	92	6.80	72.250	0	4.14	14.687	1000
2o	0.670	131	6.17	50.799	2	4.29	87.547	1000
2p	0.043	1194	7.37	33.225	2	4.48	51.124	500
2q	0.029	4250	7.54	81.575	2	4.09	122.724	500
2r	0.049	1641	7.31	26.064	3	4.58	80.536	500
2s	0.038	2166	7.42	75.763	1	4.12	83.229	1000
4a	2.755	22	5.56	0.318	193	6.50	61.551	500
4b	0.686	28	6.16	0.503	38	6.30	19.189	500
4c	1.762	21	5.75	0.790	47	6.10	36.997	500
4d	2.307	17	5.64	1.744	22	5.76	38.379	500
4e	2.006	2	5.70	0.522	8	6.28	3.944	2000
5a	3.804	3	5.42	1.884	6	5.72	10.769	500
5b	1.457	1	5.84	1.962	1	5.71	2.004	500
5c	2.314	0	5.64	9.414	0	5.03	0.805	500

¹ *P. falciparum*, strain NF54, erythrocytic stages; ² SI is defined as the ratio: IC₅₀ in L6 cells/IC₅₀ in each parasite; ³ *T. brucei rhodesiense*, strain STIB900 trypomastigote bloodstream forms; ⁴ cytotoxicity L6 cells rat skeletal myoblasts; ⁵ pIC₅₀ = $-\log_{10}$ IC₅₀ (M); ⁶ The oral toxicity was calculated using the ProTox 3.0 software (<https://tox.charite.de/protox3/>), accessed on 25 October 2024), and the calculated median lethal dose (LD₅₀) is given in mg/kg body weight. Reference drugs: chloroquine (chl.), melarsoprol (mel.), podophyllotoxin (pod.). Values in bold highlight the most striking results.

Toxicity prediction was performed using the online platform ProTox-3.0 [39], a web-based service that allows prediction of toxicity using different machine-learning models. These calculations predicted low acute oral toxicity for our compounds with LD₅₀ values not lower than 500 mg/kg. The antiplasmodial top performer **2e** together with **2f** and **4e** achieved herein the best result with a calculated LD₅₀ of 2000 mg/kg. Therefore, substituted 2-benzyl-naphthoquinone derivatives may have a high potential for the development of new antiprotozoal drugs [40].

2.3. Physicochemical Investigations

Calculated physicochemical parameters play a pivotal role in drug development, as they help to assess the pharmacological profiles of candidates for new drugs in terms of pharmacokinetics, efficacy, and safety [41–43]. The fundamental work of Lipinski et al. [44,45], who established the ‘rule of five’, provides a framework for evaluating the drug suitability of compounds based on their physicochemical properties and emphasizes the importance of these parameters in the early stages of drug discovery. For this reason, all tested compounds were subjected to a detailed drug suitability evaluation, and a number of physicochemical parameters were calculated. All synthesized compounds have relatively low molecular weights (from 248 to 402 g mol^{−1}), and the logD values (at pH 7.4) are

also suitable [38]. Furthermore, they fulfill the drug-likeness criteria proposed by Lipinski et al. [44,45] and Veber et al. [46].

Efficacy and physicochemical properties must be given equal consideration in drug development [47–50]. In recent years, ligand efficiency indices and multi-parameter scores such as ligand efficiency metrics (LE), lipophilic ligand efficiency (LLE), and binding efficiency indices (BEI) have proven to be useful tools in lead discovery and optimization, thus providing a benchmark for assessing the pharmacological value of small molecules [51–55].

However, ligand efficiency (LE) is not the best choice to find a drug candidate across a wide range of ligand sizes. In certain cases, size-independent metrics such as SILE (size-independent ligand efficiency) should be preferred [51,56,57]. While Lipinski's Rule of 5 (Ro5) describes the chemical space with the highest probability of good oral absorption, there is now increasing interest in new therapeutic agents that may not strictly follow this rule (bRo5) [43,49,58,59]. This requires more advanced tools such as the AbbVie Multi-Parameter Score (Abb-MPS) [60] or the Property Forecast Index (PFI) [61].

We have calculated the main physicochemical parameters, ligand efficiency indices and multi-parameter scores of our tested compounds and have listed them in Tables S1 and S2 in the Supplementary Materials.

2.4. Structure–Activity Relationships (SAR) of the Antiplasmodial Activity

Nearly all the compounds in this study met AB-MPS [60], PFI [61], CNS multi-parameter optimization (CNS-MPO) [62,63], and Quantitative estimate of drug-likeness (QED) [64,65] recommendations.

Most remarkable was the strong correlation of some of the calculated ligand efficiency metrics (especially size-independent ligand efficiency (SILE)) with the obtained antiplasmodial activity of our synthesized compounds (e.g., $SILE_{P.f.}$, $\rho = -0.95$; $LLE_{P.f.}$, $\rho = -0.75$). The Spearman correlation (ρ) used for this purpose is robust against outliers, as it evaluates the relationship between two variables without assuming a linear association or requiring normally distributed data. Interestingly, other size-independent ligand efficiency metrics such as ligand efficiency lipophilic price (LELP) [51] or Astex lipophilic ligand efficiency (LLE_{AT}) [66] showed no notable correlation with the efficacy of our substances.

Closer examination of LLE and SILE values of our benzylnaphthoquinone derivatives revealed a clear clustering of compounds with similar structural elements and their respective antiplasmodial activities (Figure 2 and Figure S1 in the Supplementary Materials).

The 3-(trifluoromethyl)-NQs (**5a–c**) located in the lower left corner of the plot show the least exciting values of $LLE < 1.2$, $SILE < 2.2$ and $pIC_{50} \leq 5.8$. The NQ derivatives (**4a–e**) also showed a rather low level of activity against *P. falciparum* and SILE values ≤ 2.4 . Among the menadione derivatives, only the 4,4,4-trifluorobutanamidobenzyl menadione **2o** displayed comparably poor levels (with a pIC_{50} of 6.2). All other benzylmenadione derivatives, especially the polyfluorinated ones, are highly effective (pIC_{50} in most cases ≥ 7) and lie in the upper right quadrant.

The trajectories of selected compounds in LLE and SILE space are also visualized in Figure 2. The concept of trajectory mapping provides an excellent strategic framework to evaluate the optimization process in drug development [67]. For example, the introduction of a methyl group into the NQ backbone (**4b**→**2b**, **4e**→**2f**) leads to a significant increase in potency, as indicated by a clear shift towards the north-eastern part of the SILE-LLE region. Inserting a CF_3 group, on the other hand (**4a**→**5a**, **4b**→**5b**, **4c**→**5c**), tends to reduce efficiency (shift to the bottom left). Furthermore, it can easily be deduced how the efficacy of the model substance plasmodione (**2b**) can be enhanced by further fluorination and subsequent rearrangement of the fluorinated building blocks (**2b**→**2c**→**2e**). These results

underline the benefit of the SILE vs. LLE plot as very useful for assessing the efficacy of different functional groups and residues in a drug development process.

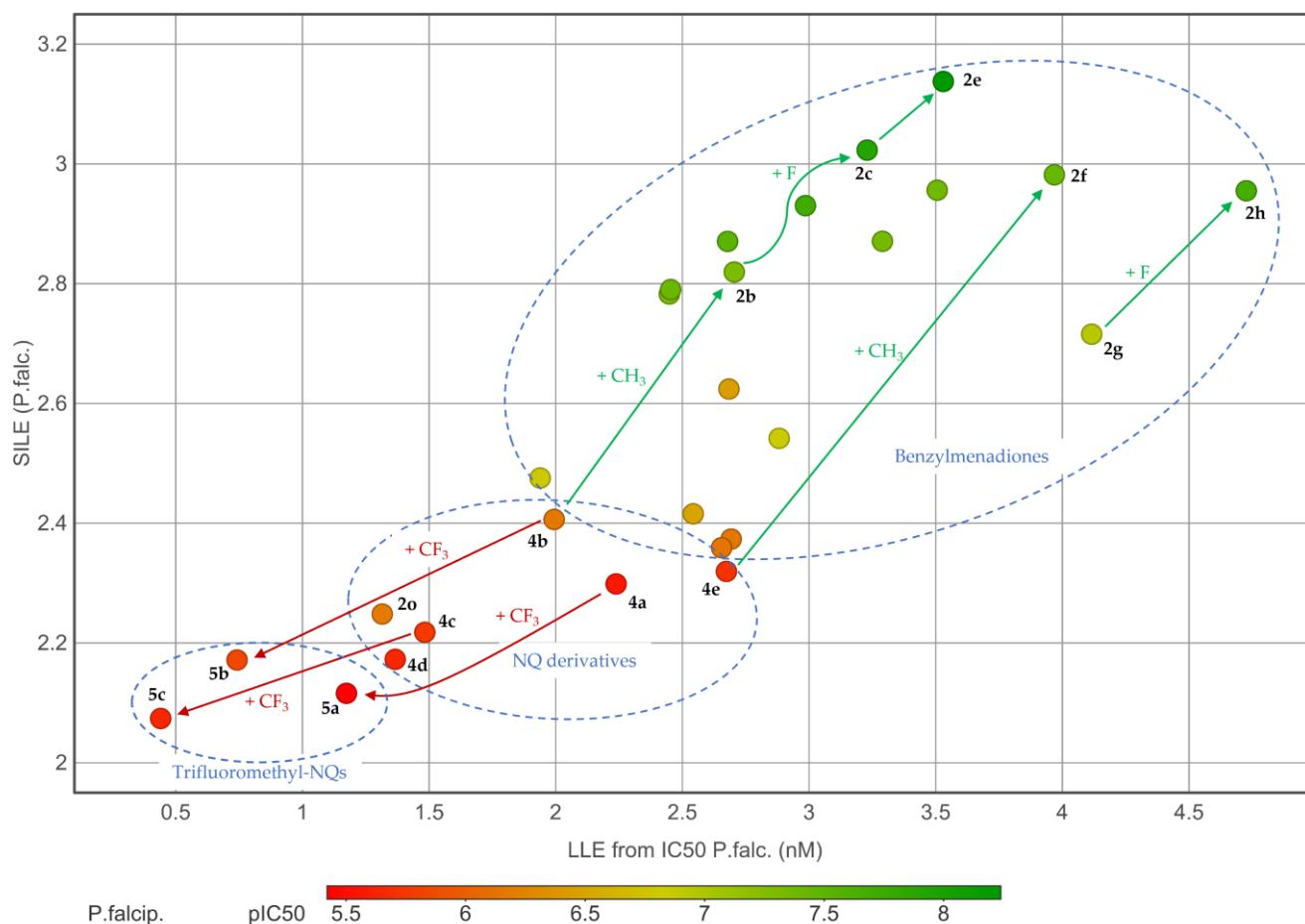


Figure 2. Scatterplot of lipophilic ligand efficiency (LLE) vs. size-independent ligand efficiency (SILE) for the synthesized compounds including some optimization trajectories; the colors are assigned according to their respective pIC₅₀.

Abad-Zapatero et al. describe an equally useful mathematical approach that integrates different ligand efficiency indices (LEIs) and defines binding affinity as a function of ligand size (usually expressed as binding affinity per non-hydrogen atom or per molecular weight) and polarity [55,68]. The application of LEIs goes beyond simple efficacy assessment; they are an important tool for Cartesian mapping of chemical–biological space, a concept referred to as AtlasCBS [69]. This mapping allows the identification and visualization of promising drug candidates and the comparison of different ligands for various targets. The pair of variables (NSEI, *n*BEI) is particularly useful to determine the ‘direction’ of the optimization path, which is specified by the corresponding framework. In the NSEI-*n*BEI plot, the compounds appear along a series of lines with slopes equal to NPOL (number of polar atoms). The most efficient compounds in terms of size and polarity are found in the north-eastern region of the plane and are therefore considered the more promising candidates for further drug development.

The application of AtlasCBS to our synthesized compounds gave a very similar result to the LLE/SILE scatterplot (Figure 2). Again, the potent polyfluorinated menadione derivatives were located in the preferred northeastern part of the NSEI-*n*BEI plane, with 2e leading the way, while the less potent NQ and 3-trifluoro-NQ derivatives tended to be found in the lower left region (Figure 3 and Figure S2 in the Supplementary Materials).

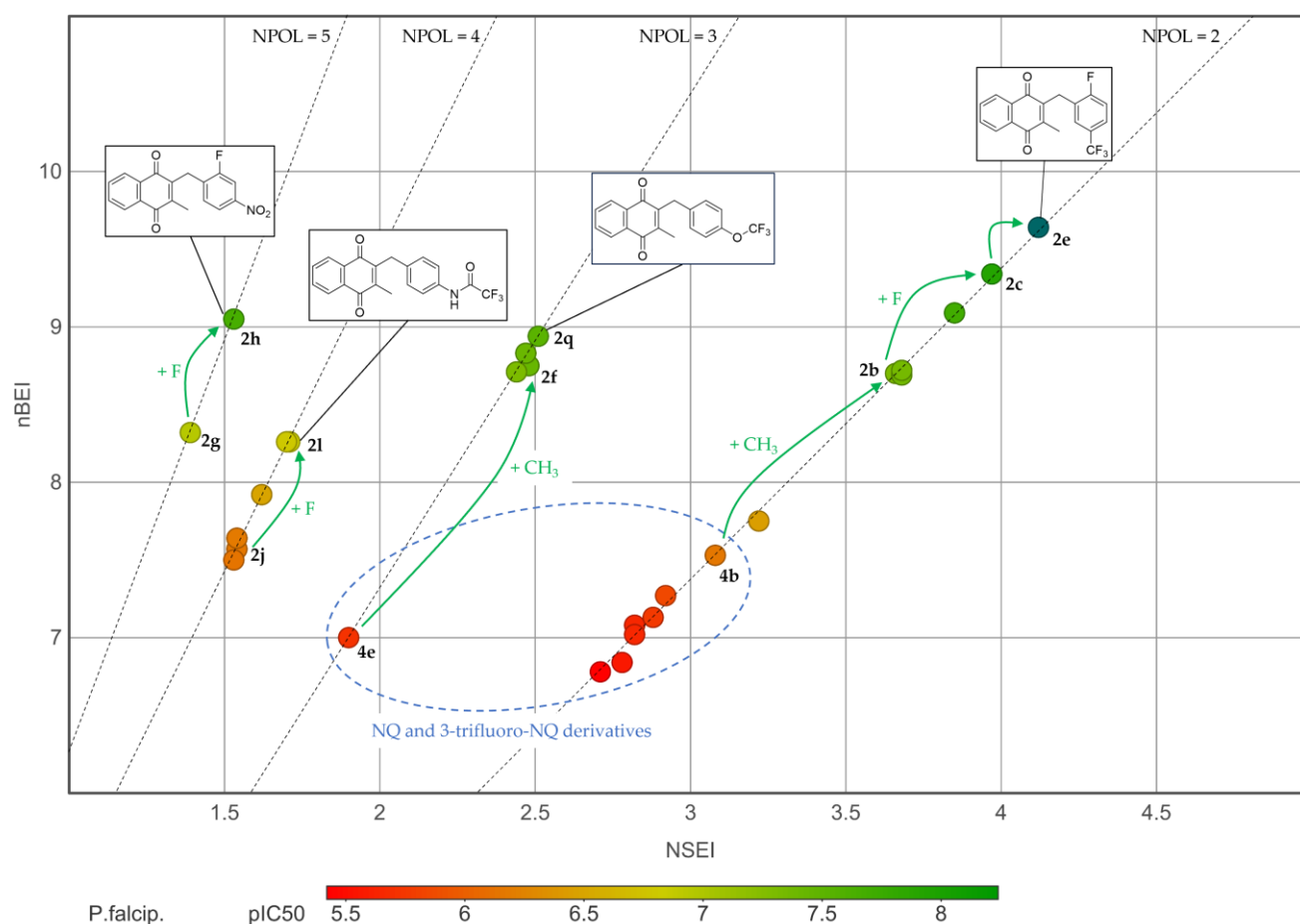


Figure 3. Application of the AtlasCBS concept using a schematic NSEI-*n*BEI plane analysis of the synthesized benzyl-naphthoquinones including optimization trajectories; the colors are assigned according to their respective pIC_{50} .

The concept of trajectory mapping can also be applied very well to the NSEI/*n*BEI plot; the increase in efficiency due to the introduction of a methyl group in the NQ backbone (**4b**→**2b**, **4e**→**2f**), as well as the introduction of fluorine atoms (**2g**→**2h**; **2j**→**2l**; **2b**→**2c**→**2e**) are clearly reflected by a significant shift towards the preferred northeastern part of the NSEI-*n*BEI plane.

The excellent potential of (poly)fluorinated menadiones for the development of new antiplasmodial agents is also reflected in the SILE/log SI correlation plot (Figure 4 and Figure S3 in the Supplementary Materials), where most of these compounds showed more than 300-fold selectivity ($\log SI > 2.5$) between the IC_{50} for the rat L6 skeletal cell line and the IC_{50} for *Plasmodium falc.*, as well as adequate ligand efficiency indices. Compounds with $SI > \sim 300$ and pIC_{50} values greater than 7 (corresponding to activity < 0.1 mM) combine high activity with acceptable selectivity against an L6 cell line and are thus considered promising drug candidates for further studies [36–38]. However, the SILE/log SI scatterplot also proves that (even fluorinated) menadiones with an acid amide moiety **2j**–**o** do not lead to acceptable results.

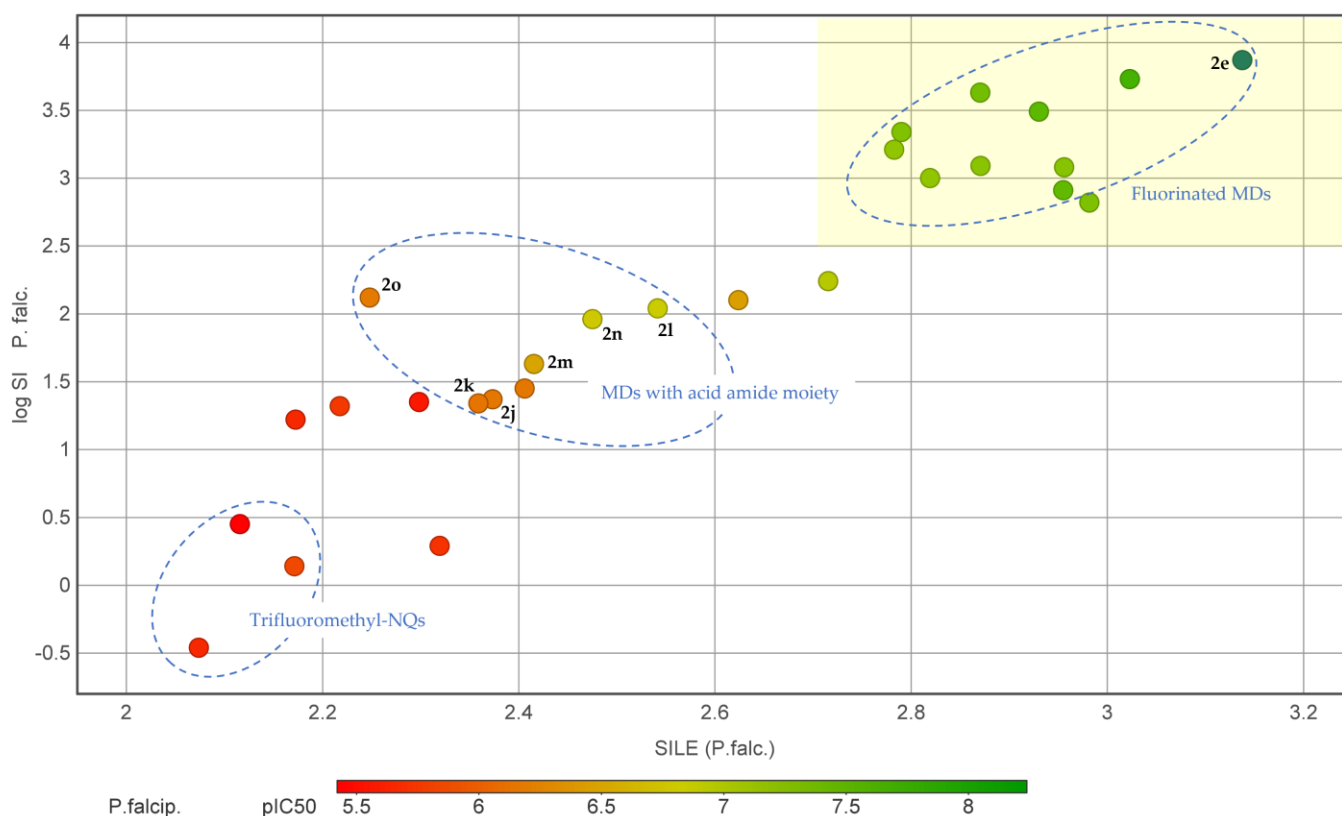


Figure 4. Plot of SILE (*P. falciparum*) data obtained in this study (x) vs. calculated log SI (*P. falciparum*) (y); the colors are assigned according to their respective pIC₅₀. Substances that lie in the yellow shaded area combined high selectivity with acceptable size-independent ligand efficiency values.

3. Materials and Methods

3.1. Chemistry

3.1.1. General Information

All reagents and solvents were obtained from Merck and Fluorochem Ltd. (Pune, India) Moisture-sensitive reactions were performed under an inert argon atmosphere. Each reaction was monitored by TLC on Merck TLC plates (silica gel 60 F254 0.2 mm, 200 × 200 mm) and detected at 254 nm. All reaction products were purified by flash column chromatography on silica gel 60 (Merck, Darmstadt, Germany, 70–230 mesh, pore diameter 60 Å) unless otherwise stated. Purity and homogeneity of the final compounds were checked by TLC and high-resolution mass spectrometry. Melting points were determined using a digital melting point meter (Electrothermal IA 9200, Thermo Fisher Scientific, Birmingham, UK). Microwave-assisted reactions were carried out in a CEM Discover/Explorer system in sealed 10 cm³ standard vessels with temperature control.

Accurate structural elucidation was confirmed by 1D and 2D NMR spectroscopy on a Bruker Avance Neo 400 MHz instrument (at 298 K) using 5 mm tubes. Chemical shifts were expressed in δ (ppm) using either tetramethylsilane (TMS) or the ¹³C signal of the solvents (CDCl₃ δ 77.04 ppm, DMSO-*d*₆ δ 39.45 ppm) as the internal standard. ¹H and ¹³C resonances were numbered according to the formulae (see Supplementary Materials); signals marked with an asterisk are interchangeable.

ESI and APCI mass spectra were acquired by analyzing sample solutions on an Ultimate 3000 HPLC with a Q Exactive™ Hybrid Quadrupole-Orbitrap™ mass spectrometer equipped with a heated ESI II source or an APCI source (Thermo Fisher Scientific, Birmingham, UK) in positive or negative ionization mode.

3.1.2. General Synthetic Procedure for Benzylmenadiones **2a–i** (Route A)

Menadione (1.0 mmol) was added to a stirred solution of the respective phenylacetic acid derivative (1.4 equiv.) in CH₃CN (9 mL) and H₂O (3 mL) and heated to 85 °C. AgNO₃ (0.35 equiv.) was added first and then (NH₄)₂S₂O₈ (1.3 equiv.) dissolved in 4 mL CH₃CN/H₂O (3:1) dropwise over a period of 5 min. Stirring at 85 °C was continued until TLC showed complete consumption of the starting material (1–4 h). After cooling to ambient temperature, the mixture was extracted three times with CH₂Cl₂ (20 mL). The combined organic layers were washed with H₂O, dried over Na₂SO₄, and concentrated in vacuo to give a residue, which was purified by flash chromatography as detailed below.

2-Benzyl-3-methyl-1,4-naphthoquinone (2a). Compound **2a** was obtained after stirring for 1 h, then purified by flash chromatography using toluene/cyclohexane (15:1). Yellow solid; yield: 88%; *R*_f = 0.50 (toluene:cyclohexane = 15:1); m.p.: 104–106 °C (lit [28] m.p. 105–106 °C). The spectroscopic data were found to be identical to the ones described in [28]. Although **2a** represents an already known compound, to our knowledge the complete assignment of the NMR signals has not been published so far: ¹H NMR (400 MHz, CDCl₃) δ = 8.09 (m, 2H, H-8, H-5), 7.69 (m, 2H, H-6, H-7), 7.26 (m, 4H, H-2', H-3', H-5', H-6'), 7.19 (m, 1H, H-4'), 4.03 (s, 2H, H-9), 2.25 (s, 3H, H-10) ppm; ¹³C NMR (100 MHz, CDCl₃): δ = 185.4 (C-4), 184.7 (C-1), 145.3 (C-3), 144.4 (C-2), 138.0 (C-1'), 133.5 (C-6, C-7), 132.1 (C-4a), 132.0 (C-8a), 128.6 (C-2', C-3', C-5', C-6'), 126.5 (C-5), 126.4 (C-4'), 126.3 (C-8), 32.4 (C-9), 13.3 (C-10) ppm.

2-Methyl-3-[[4-(trifluoromethyl)phenyl]methyl]-1,4-naphthoquinone (2b). Compound **2b** was obtained after stirring for 1.5 h, then purified by flash chromatography using toluene/cyclohexane (15:1). Yellow solid; yield: 83%; *R*_f = 0.42 (toluene:cyclohexane = 15:1); m.p.: 70–71 °C (lit [28] m.p. 70–71 °C). The spectroscopic data were found to be identical to the ones described in [28]. Although **2b** represents an already known compound, to our knowledge the complete assignment of the NMR signals has not been published so far: ¹H NMR (400 MHz, DMSO-*d*₆) δ = 7.98 (m, 2H, H-5, H-8), 7.82 (m, 2H, H-6, H-7), 7.60 (d, *J* = 7.8 Hz, 2H, H-3', H-5'), 7.45 (d, *J* = 7.8 Hz, 2H, H-2', H-6'), 4.06 (s, 2H, H-9), 2.14 (s, 3H, H-10) ppm; ¹³C NMR (100 MHz, DMSO-*d*₆) δ = 184.4 (C-4), 183.9 (C-1), 144.8* (C-2), 143.4* (C-3), 143.2 (C-1'), 133.9* (C-6), 133.8* (C-7), 131.6* (C-4a), 131.3* (C-8a), 129.2 (C-2', C-6'), 126.9 (q, ²*J*_{C,F} = 31.8 Hz, C-4'), 125.9* (C-5), 125.8* (C-8), 125.2 (q, ³*J*_{C,F} = 3.9 Hz, C-3', C-5'), 124.2 (q, ¹*J*_{C,F} = 271.9 Hz, CF₃), 31.6 (C-9), 13.0 (C-10) ppm.

2-[[2-Fluoro-4-(trifluoromethyl)phenyl]methyl]-3-methyl-1,4-naphthoquinone (2c). Compound **2c** was obtained after stirring for 3 h, then purified by flash chromatography using toluene/cyclohexane (15:1). Yellow solid; yield: 69%; *R*_f = 0.48 (toluene:cyclohexane = 15:1); m.p.: 86–87 °C. ¹H NMR (400 MHz, CDCl₃) δ = 8.10 (m, 2H, H-5, H-8), 7.72 (m, 2H, H-6, H-7), 7.31 (m, 3H, H-3', H-5', H-6'), 4.09 (s, 2H, H-9), 2.23 (s, 3H, H-10) ppm; ¹³C NMR (100 MHz, CDCl₃) δ = 184.9 (C-4), 184.3 (C-1), 160.4 (d, ¹*J*_{C,F} = 248.2 Hz, C-2'), 145.6 (C-3), 143.2 (C-2), 133.7 (C-6, C-7), 132.1 (C-4a), 131.9 (C-8a), 131.1 (d, ³*J*_{C,F} = 4.4 Hz, C-6'), 130.7 (qd, ²*J*_{C,F} = 33.4, ³*J*_{C,F} = 8.0 Hz, C-4'), 129.2 (d, ²*J*_{C,F} = 15.5 Hz, C-1'), 126.5 (C-5, C-8), 123.7 (qd, ¹*J*_{C,F} = 272.1, ⁴*J*_{C,F} = 2.5 Hz, CF₃), 121.1 (C-5'), 112.9 (dq, ²*J*_{C,F} = 25.7, ³*J*_{C,F} = 3.8 Hz, C-3'), 25.7 (C-9), 13.1 (C-10) ppm; HRMS (APCI) calcd. for C₁₉H₁₂F₄O₂ [M][−] = 348.0773; found: 348.0783.

2-[[4-Fluoro-2-(trifluoromethyl)phenyl]methyl]-3-methyl-1,4-naphthoquinone (2d). Compound **2d** was obtained after stirring for 3 h, then purified by flash chromatography using toluene/cyclohexane (15:1). Yellow solid; yield: 66%; *R*_f = 0.50 (toluene:cyclohexane = 15:1); m.p.: 86–87 °C. ¹H NMR (400 MHz, DMSO-*d*₆) δ = 8.06 (m, 1H, H-5), 7.98 (m, 1H, H-8), 7.85 (m, 2H, H-6, H-7), 7.64 (dd, *J* = 9.3, 2.7 Hz, 1H, H-3'), 7.33 (td, *J* = 8.4, 2.7 Hz, 1H, H-5'), 7.28 (m, 1H, H-6'), 4.07 (s, 2H, H-9), 2.05 (s, 3H, H-10) ppm; ¹³C NMR (100 MHz, DMSO-*d*₆) δ = 184.3 (C-4), 183.8 (C-1), 160.1 (d, ¹*J*_{C,F} = 244.8 Hz, C-4'), 146.1 (C-3), 142.3 (C-2), 133.9

(C-6), 133.8 (C-7), 132.5 (C-1'), 131.9 (C-4a), 131.5 (C-8a), 131.1 (d, $^3J_{C,F}$ = 8.0 Hz, C-6'), 128.5 (qd, $^2J_{C,F}$ = 30.6, $^3J_{C,F}$ = 7.6 Hz, C-2'), 125.9 (C-5, C-8), 123.6 (qd, $^1J_{C,F}$ = 274.3, $^4J_{C,F}$ = 2.8 Hz, CF₃), 119.4 (d, $^2J_{C,F}$ = 20.3 Hz, C-5'), 113.7 (dq, $^2J_{C,F}$ = 25.4, $^3J_{C,F}$ = 6.0 Hz, C-3'), 27.8 (C-9), 12.8 (C-10) ppm; HRMS (APCI) calcd. for C₁₉H₁₂F₄O₂ [M][−] = 348.0773; found: 348.0784.

2-[[2-Fluoro-5-(trifluoromethyl)phenyl]methyl]-3-methyl-1,4-naphthoquinone (**2e**). Compound **2e** was obtained after stirring for 3.5 h, then purified by flash chromatography using toluene/cyclohexane (15:1). Yellow solid; yield: 63%; R_f = 0.44 (toluene:cyclohexane = 15:1); m.p.: 88–89 °C. ¹H NMR (400 MHz, DMSO-*d*₆) δ = 8.02 (m, 1H, H-5), 7.98 (m, 1H, H-8), 7.84 (m, 2H, H-6, H-7), 7.66 (m, 2H, H-4', H-6'), 7.42 (t, J = 9.2 Hz, 1H, H-3'), 4.05 (s, 2H, H-9), 2.14 (s, 3H, H-10) ppm; ¹³C NMR (100 MHz, DMSO-*d*₆) δ = 184.4 (C-4), 183.8 (C-1), 162.3 (dq, $^1J_{C,F}$ = 250.4, 1.5 Hz, C-2'), 145.4* (C-3), 142.1* (C-2), 133.7 (C-6, C-7), 131.8* (C-4a), 131.5* (C-8a), 127.7 (C-6'), 127.1 (C-1'), 125.9 (C-4'), 125.8 (C-5, C-8), 125.3 (qd, $^2J_{C,F}$ = 32.3, $^4J_{C,F}$ = 3.3 Hz, C-5'), 123.7 (q, $^1J_{C,F}$ = 271.1 Hz, CF₃), 116.3 (d, $^2J_{C,F}$ = 23.8 Hz, C-3'), 25.4 (C-9), 12.9 (C-10) ppm; HRMS (ESI) calcd. for C₁₉H₁₁F₄O₂ [M-H][−] = 347.0695; found: 347.0703.

2-[(6-Chloropyridin-3-yl)methyl]-3-methyl-1,4-naphthoquinone (**2f**). Compound **2f** was obtained after stirring for 3 h, then purified by flash chromatography using toluene/cyclohexane (15:1). Yellow solid; yield: 60%; R_f = 0.48 (toluene:cyclohexane = 15:1); m.p.: 159–160 °C. ¹H NMR (400 MHz, DMSO-*d*₆) δ = 8.35 (dd, J = 2.5, 0.8 Hz, 1H, H-2'), 8.00 (m, 2H, H-5, H-8), 7.84 (m, 2H, H-6, H-7), 7.71 (dd, J = 8.3, 2.6 Hz, 1H, H-4'), 7.40 (dd, J = 8.3, 0.7 Hz, 1H, H-5'), 4.00 (s, 2H, H-9), 2.18 (s, 3H, H-10) ppm; ¹³C NMR (100 MHz, DMSO-*d*₆) δ = 184.4 (C-4), 184.0 (C-1), 149.7 (C-2'), 148.0 (C-6'), 145.0 (C-3), 142.9 (C-2), 139.6 (C-4'), 133.9* (C-7), 133.8* (C-6), 133.7 (C-3'), 131.7 (C-8a), 131.4 (C-4a), 125.9* (C-5), 125.8* (C-8), 124.0 (C-5'), 28.5 (C-9), 13.0 (C-10) ppm; HRMS (ESI) calcd. for C₁₇H₁₃ClNO₂ [M+H]⁺ = 298.0635; found: 298.0627.

2-Methyl-3-[(4-nitrophenyl)methyl]-1,4-naphthoquinone (**2g**). Compound **2g** was obtained after stirring for 2.5 h, then purified by flash chromatography using toluene/cyclohexane (15:1). Yellow solid; yield: 66%; R_f = 0.40 (toluene:cyclohexane = 15:1); m.p.: 160–161 °C (lit [18] m.p. 156–157 °C). The spectroscopic data were found to be identical to the ones described in [18,28]. Although **2g** represents an already known compound, to our knowledge the complete assignment of the NMR signals has not been published so far: ¹H NMR (400 MHz, DMSO-*d*₆) δ = 8.13 (d, J = 8.8 Hz, 2H, H-2', H-6'), 8.02 (m, 2H, H-5, H-8), 7.85 (m, 2H, H-6, H-7), 7.53 (d, J = 8.8 Hz, 2H, H-3', H-5'), 4.13 (s, 2H, H-9), 2.16 (s, 3H, H-10) ppm; ¹³C NMR (100 MHz, DMSO-*d*₆) δ = 184.5 (C-4), 183.9 (C-1), 146.6 (C-4'), 145.9 (C-1'), 145.2 (C-3), 143.1 (C-2), 133.9 (C-6, C-7), 131.7* (C-4a), 131.4* (C-8a), 129.5 (C-3', C-5'), 125.9 (C-5, C-8), 123.5 (C-2', C-6'), 31.7 (C-9), 13.1 (C-10) ppm.

2-[(2-Fluoro-4-nitrophenyl)methyl]-3-methyl-1,4-naphthoquinone (**2h**). Compound **2h** was obtained after stirring for 3 h, then purified by flash chromatography using toluene/cyclohexane (15:1). Yellow solid; yield: 58%; R_f = 0.48 (toluene:cyclohexane = 15:1); m.p.: 170–171 °C. ¹H NMR (400 MHz, DMSO-*d*₆) δ = 8.10 (dd, J = 9.9, 2.4 Hz, 1H, H-3'), 8.04 (m, 1H, H-5), 7.98 (m, 1H, H-8), 7.95 (m, 1H, H-5'), 7.85 (m, 2H, H-6, H-7), 7.53 (dd, J = 8.5, 7.7 Hz, 1H, H-6'), 4.09 (s, 2H, H-9), 2.15 (s, 3H, H-10) ppm; ¹³C NMR (100 MHz, DMSO-*d*₆) δ = 184.3 (C-4), 183.6 (C-1), 159.4 (d, $^1J_{C,F}$ = 248.7 Hz, C-2'), 146.8 (d, $^3J_{C,F}$ = 9.1 Hz, C-4'), 145.8 (C-3), 141.9 (C-2), 134.0 (C-7), 133.9 (C-6), 133.5 (d, $^2J_{C,F}$ = 15.8 Hz, C-1'), 131.7 (C-4a), 131.4 (C-8a), 131.0 (d, $^3J_{C,F}$ = 4.6 Hz, C-6'), 125.9 (C-5, C-8), 119.5 (d, $^4J_{C,F}$ = 3.4 Hz, C-5'), 110.9 (d, $^2J_{C,F}$ = 27.6 Hz, C-3'), 25.6 (d, $^3J_{C,F}$ = 2.8 Hz, C-9), 13.0 (C-10) ppm; HRMS (ESI) calcd. for C₁₈H₁₁FNO₄ [M-H][−] = 324.0672; found: 324.0680.

2-Methyl-3-[(2,4,5-trifluorophenyl)methyl]-1,4-naphthoquinone (**2i**). Compound **2i** was obtained after stirring for 4 h, then purified by flash chromatography using toluene/cyclohexane (15:1). Yellow solid; yield: 55%; R_f = 0.39 (toluene:cyclohexane = 15:1); m.p.: 159–160 °C.

^1H NMR (400 MHz, DMSO- d_6) δ = 8.02 (m, 1H, H-5), 7.97 (m, 1H, H-8), 7.84 (m, 2H, H-6, H-7), 7.51 (ddd, J = 10.9, 9.7, 6.9 Hz, 1H, H-3'), 7.36 (ddd, J = 11.5, 9.0, 7.1 Hz, 1H, H-6') 3.92 (s, 2H, H-9), 2.11 (s, 3H, H-10) ppm; ^{13}C NMR (100 MHz, DMSO- d_6) δ = 184.3 (C-4), 183.7 (C-1), 155.2 (ddd, $^1J_{\text{C,F}}$ = 243.2, $^3J_{\text{C,F}}$ = 9.8, $^4J_{\text{C,F}}$ = 2.3 Hz, C-2'), 147.8 (ddd, $^1J_{\text{C,F}}$ = 246.7, $^2J_{\text{C,F}}$ = 14.3, $^3J_{\text{C,F}}$ = 13.0 Hz, C-4'), 146.0 (ddd, $^1J_{\text{C,F}}$ = 241.6, $^2J_{\text{C,F}}$ = 12.4, $^4J_{\text{C,F}}$ = 3.5 Hz, C-5'), 145.6 (C-3), 141.9 (C-2), 133.8* (C-6), 133.7* (C-7), 131.8 (C-4a), 131.5 (C-8a), 125.9* (C-5), 125.8* (C-8), 122.2 (ddd, $^2J_{\text{C,F}}$ = 18.1, $^3J_{\text{C,F}}$ = 5.9, $^4J_{\text{C,F}}$ = 4.0 Hz, C-1'), 117.8 (dd, $^2J_{\text{C,F}}$ = 19.8, $^3J_{\text{C,F}}$ = 5.7 Hz, C-6'), 105.6 (dd, $^2J_{\text{C,F}}$ = 29.1, $^3J_{\text{C,F}}$ = 21.3 Hz, C-3'), 24.7 (d, $^3J_{\text{C,F}}$ = 2.9 Hz, C-9), 12.8 (C-10) ppm; HRMS (APCI) calcd. for $\text{C}_{18}\text{H}_{11}\text{F}_3\text{O}_2$ $[\text{M}]^-$ = 316.0711; found: 316.0721.

3.1.3. General Synthetic Procedure for Acetamidobenzylmenadiones **2j,k** (Route C)

The respective aminophenylacetic acid (200 mg) was added to glacial acetic acid (3 mL) and subjected to microwave irradiation (180 W, 150 °C) for 40 min. The reaction mixture was poured into EtOAc (50 mL) and washed with H_2O (15 mL) three times. The combined organic layers were dried over Na_2SO_4 and concentrated in vacuo to yield the crude products as orange solids, which were used without further purification.

As described in the Section 3.1.2, menadione (1 equiv.) was then added to a stirred solution of the above acetaminophenylacetic acid (2 equiv.) and treated with AgNO_3 and $(\text{NH}_4)_2\text{S}_2\text{O}_8$ to give the corresponding acetamidobenzylmenadiones.

2-[(4-Acetamidophenyl)methyl]-3-methyl-1,4-naphthoquinone (2j). Compound **2j** was obtained after stirring for 1.5 h, then purified by flash chromatography using toluene/cyclohexane (15:1). Yellow solid; yield: 94%; R_f = 0.41 (toluene:cyclohexane = 15:1); m.p.: 196–197 °C (lit [35] m.p. 198–200 °C). The spectroscopic data were found to be identical to the ones described in [35]. Although **2j** represents an already known compound, to our knowledge the complete assignment of the NMR signals has not been published so far: ^1H NMR (400 MHz, DMSO- d_6) δ = 9.85 (s, 1H, NH), 8.00 (m, 2H, H-5, H-8), 7.83 (m, 2H, H-6, H-7), 7.45 (d, J = 8.6 Hz, 2H, H-3', H-5'), 7.13 (d, J = 8.6 Hz, 2H, H-2', H-6'), 3.92 (s, 2H, H-9), 2.14 (s, 3H, H-10), 1.99 (s, 3H, $\text{CH}_3\text{-CO}$) ppm; ^{13}C NMR (100 MHz, DMSO- d_6) δ = 184.7 (C-4), 184.1 (C-1), 168.0 (CO- CH_3), 144.5* (C-2), 144.1* (C-3), 137.4 (C-4'), 133.9* (C-6), 133.8* (C-7), 132.5 (C-1'), 131.6* (C-4a), 131.4* (C-8a), 128.5 (C-2', C-6'), 125.9* (C-5), 125.8* (C-8), 119.1 (C-3', C-5'), 31.0 (C-9), 23.8 ($\text{CH}_3\text{-CO}$), 12.9 (C-10) ppm.

2-[(3-Acetamidophenyl)methyl]-3-methyl-1,4-naphthoquinone (2k). Compound **2k** was obtained after stirring for 1.5 h, then purified by flash chromatography using toluene/cyclohexane (15:1). Yellow solid; yield: 90%; R_f = 0.41 (toluene:cyclohexane = 15:1); m.p.: 188–189 °C (lit [35] m.p. 163–165 °C). The spectroscopic data were found to be identical to the ones described in [35]. Although **2k** represents an already known compound, to our knowledge the complete assignment of the NMR signals has not been published so far: ^1H NMR (400 MHz, DMSO- d_6) δ = 9.81 (s, 1H, NH), 8.01 (m, 2H, H-5, H-8), 7.84 (m, 2H, H-6, H-7), 7.49 (ddd, J = 8.2, 2.2, 1.1 Hz, 1H, H-4'), 7.31 (t, J = 1.9 Hz, 1H, H-2'), 7.18 (t, J = 7.8 Hz, 1H, H-5'), 6.91 (m, 1H, H-6'), 3.95 (s, 2H, H-9), 2.15 (s, 3H, H-10), 1.98 (s, 3H, $\text{CH}_3\text{-CO}$) ppm; ^{13}C NMR (100 MHz, DMSO- d_6) δ = 184.6 (C-4), 183.9 (C-1), 168.1 (CO- CH_3), 144.4* (C-2), 144.3* (C-3), 139.5 (C-3'), 138.5 (C-1'), 133.9 (C-6, C-7), 131.6* (C-4a), 131.4* (C-8a), 128.7 (C-5'), 126.0* (C-5), 125.8* (C-8), 118.4 (C-2'), 116.8 (C-4'), 123.1 (C-6'), 31.6 (C-9), 23.9 ($\text{CH}_3\text{-CO}$), 12.9 (C-10) ppm.

3.1.4. General Synthetic Procedure for Amidobenzylmenadiones **2l-o** (Route C)

The acetamido derivatives **2j** resp. **2k** (200 mg) were added to a mixture of HCl conc. (0.5 mL) and MeOH (4 mL) and subjected to microwave irradiation (250 W, 150 °C) for 30 min. The reaction mixture was poured into EtOAc (50 mL) and washed with sat. aq Na_2CO_3 (15 mL) three times. The combined organic layers were dried over Na_2SO_4 and

concentrated in vacuo to obtain crude products as orange solids, which were used without further purification.

The above prepared unprotected aminobenzyl derivative (1 equiv.) and dicyclohexylcarbodiimide (DCC, 1.2 equiv.) were added in sequence to a stirred solution of the corresponding carboxylic acid (1.25 mmol, 1 equiv.) in anhydrous DMF (4 mL) under exclusion of air or humidity. The reaction mixture was stirred at rt until TLC showed complete consumption of the starting material (3–4 h). The mixture was then filtered and the residue extracted with MTBE (20 mL). The combined organic layers were washed successively with H₂O, 1M HCl, and sat. aq Na₂CO₃, dried over Na₂SO₄, and concentrated in vacuo to give a residue, which was purified by flash chromatography as detailed below.

2-Methyl-3-([4-(2,2,2-trifluoroacetamido)phenyl]methyl)-1,4-naphthoquinone (2l). Compound **2l** was obtained after stirring for 3 h, then purified by flash chromatography using toluene/cyclohexane (15:1). Yellow solid; yield: 71%; *R*_f = 0.51 (toluene:cyclohexane = 15:1); m.p.: 194–195 °C. ¹H NMR (400 MHz, DMSO-*d*₆) δ = 11.19 (s, 1H, NH), 8.01 (m, 2H, H-5, H-8), 7.84 (m, 2H, H-6, H-7), 7.56 (m, 2H, H-3', H-5'), 7.27 (m, 2H, H-2', H-6'), 3.98 (s, 2H, H-9), 2.16 (s, 3H, H-10) ppm; ¹³C NMR (100 MHz, DMSO-*d*₆) δ = 184.6 (C-4), 184.0 (C-1), 154.3 (q, ²*J*_{C,F} = 36.8 Hz, CO-CF₃), 144.4* (C-3), 144.1* (C-2), 135.6 (C-1'), 134.3 (C-4'), 133.9* (C-6), 133.8* (C-7), 131.7* (C-4a), 131.4* (C-8a), 128.8 (C-2', C-6'), 125.9* (C-5), 125.8* (C-8), 121.2 (C-3', C-5'), 115.7 (q, ¹*J*_{C,F} = 288.9 Hz, CF₃), 31.2 (C-9), 12.9 (C-10) ppm; HRMS (ESI) calcd. for C₂₀H₁₃F₃NO₃ [M-H][−] = 372.0848; found: 372.0854.

2-Methyl-3-([3-(2,2,2-trifluoroacetamido)phenyl]methyl)-1,4-naphthoquinone (2m). Compound **2m** was obtained after stirring for 3 h, then purified by flash chromatography using toluene/cyclohexane (15:1). Yellow solid; yield: 31%; *R*_f = 0.53 (toluene:cyclohexane = 15:1); m.p.: 194–195 °C. ¹H NMR (400 MHz, DMSO-*d*₆) δ = 11.12 (s, 1H, NH), 8.01 (m, 2H, H-5, H-8), 7.84 (m, 2H, H-6, H-7), 7.57 (ddd, *J* = 7.9, 2.2, 1.1 Hz, 1H, H-4'), 7.45 (t, *J* = 1.9 Hz, 1H, H-2'), 7.31 (t, *J* = 7.9 Hz, 1H, H-5'), 7.13 (ddd, *J* = 7.9, 1.8, 1.0 Hz, 1H, H-6'), 4.00 (s, 2H, H-9), 2.17 (s, 3H, H-10) ppm; ¹³C NMR (100 MHz, DMSO-*d*₆) δ = 184.6 (C-4), 183.9 (C-1), 154.3 (q, ²*J*_{C,F} = 37.0 Hz, CO-CF₃), 144.5* (C-2), 144.1* (C-3), 139.1 (C-1'), 136.5 (C-3'), 133.9 (C-6, C-7), 131.6* (C-4a), 131.4* (C-8a), 129.0 (C-5'), 126.0* (C-5), 125.9* (C-8), 125.8 (C-6'), 118.7 (C-4'), 120.4 (C-2'), 115.6 (q, ¹*J*_{C,F} = 288.8 Hz, CF₃), 31.6 (C-9), 13.0 (C-10) ppm; HRMS (ESI) calcd. for C₂₀H₁₃F₃NO₃ [M-H][−] = 372.0848; found: 372.0855.

2-Methyl-2-([4-(4,4,4-trifluorobutanamido)phenyl]methyl)-1,4-naphthoquinone (2n). Compound **2n** was obtained after stirring for 4 h, then purified by flash chromatography using toluene/cyclohexane (15:1). Yellow solid; yield: 70%; *R*_f = 0.40 (toluene:cyclohexane = 15:1); m.p.: 180–181 °C. ¹H NMR (400 MHz, DMSO-*d*₆) δ = 10.00 (s, 1H, NH), 8.01 (m, 2H, H-5, H-8), 7.84 (m, 2H, H-6, H-7), 7.46 (d, *J* = 8.4 Hz, 2H, H-3', H-5'), 7.16 (d, *J* = 8.4 Hz, 2H, H-2', H-6'), 3.93 (s, 2H, H-9), 2.57 (m, 4H, H-2'', H-3''), 2.15 (s, 3H, H-10) ppm; ¹³C NMR (100 MHz, DMSO-*d*₆) δ = 184.7 (C-4), 184.1 (C-1), 168.0 (C-1''), 144.5* (C-2), 144.1* (C-3), 137.1 (C-4'), 133.9* (C-6), 133.8* (C-7), 132.9 (C-1'), 131.6* (C-4a), 131.4* (C-8a), 128.6 (C-2', C-6'), 127.4 (q, ¹*J*_{C,F} = 276.2 Hz, C-4''), 125.9 (C-5, C-8), 119.2 (C-3', C-5'), 31.1 (C-9), 28.5 (C-2''), 28.4 (q, ²*J*_{C,F} = 28.7 Hz, C-3''), 12.9 (C-10) ppm; HRMS (ESI) calcd. for C₂₂H₁₇F₃NO₃ [M-H][−] = 400.1161; found: 400.1168.

2-Methyl-3-([3-(4,4,4-trifluorobutanamido)phenyl]methyl)-1,4-naphthoquinone (2o). Compound **2o** was obtained after stirring for 4 h, then purified by flash chromatography using toluene/cyclohexane (15:1). Yellow solid; yield: 16%; *R*_f = 0.42 (toluene:cyclohexane = 15:1); m.p.: 180–181 °C. ¹H NMR (400 MHz, DMSO-*d*₆) δ = 9.97 (s, 1H, NH), 8.01 (m, 2H, H-5, H-8), 7.85 (m, 2H, H-6, H-7), 7.50 (dt, *J* = 7.9, 1.3 Hz, 1H, H-4'), 7.33 (t, *J* = 1.3 Hz, 1H, H-2'), 7.21 (t, *J* = 7.9 Hz, 1H, H-5'), 6.95 (dt, *J* = 7.9, 1.3 Hz, 1H, H-6'), 3.96 (s, 2H, H-9), 2.54 (m, 2H, H-2''), 2.51 (m, 2H, H-3''), 2.16 (s, 3H, H-10) ppm; ¹³C NMR (100 MHz, DMSO-*d*₆) δ = 184.6 (C-4), 183.9 (C-1), 168.1 (C-1''), 144.4* (C-2), 144.3* (C-3), 139.1 (C-3'), 138.7 (C-1'),

134.0* (C-6), 133.9* (C-7), 131.6* (C-4a), 131.4* (C-8a), 128.8 (C-5'), 127.4 (q, $^1J_{C,F}$ = 276.2 Hz, C-4''), 126.0* (C-5), 125.9* (C-8), 123.4 (C-6'), 118.5 (C-2'), 116.9 (C-4'), 31.6 (C-9), 28.6 (q, $^3J_{C,F}$ = 2.9 Hz, C-2''), 28.3 (q, $^2J_{C,F}$ = 28.4 Hz, C-3''), 12.9 (C-10) ppm; HRMS (ESI) calcd. for $C_{22}H_{19}F_3NO_3$ $[M+H]^+$ = 402.1317; found: 402.1305.

3.1.5. General Synthetic Procedure for Benzylmenadiones **2p–s** (Route D)

Tetralone (200 mg, 1 equiv.) and the respective aldehyde (1.1 equiv.) were added successively to a stirred solution of KOH (1.2 equiv.) in EtOH (5 mL) at rt. The stirring was continued until the TLC showed complete consumption of the starting material (2.5–4 h). The mixture was poured into 30 mL of ice-cold water, and a white precipitate was formed. The product was filtered, washed with ice-cold water and concentrated in vacuo to give a beige solid, which was used without further purification.

Trichlororhodium trihydrate (0.1 equiv.) was added to a stirred solution of the benzyldene derivative prepared above (200 mg, 1 equiv.) in well-degassed EtOH (5 mL) under strict exclusion of air or moisture. The mixture was refluxed until the TLC showed complete consumption of the starting material (24 h). After concentration, the residue was partitioned between H_2O (15 mL) and EtOAc (50 mL) and the aqueous layer was extracted again with EtOAc (30 mL). The combined organic layers were dried over Na_2SO_4 and concentrated in vacuo to obtain the crude product, which was used without further purification.

(Diacetoxyiodo)benzene (PIDA) (2.1 equiv.) was added in portions to a stirred solution of above prepared naphthol (200 mg, 1 equiv.) in acetonitrile (5 mL) and water (2 mL) at $-5^\circ C$ for 20–30 min. The reaction mixture was allowed to reach ambient temperature and stirred until the TLC showed complete consumption of the starting material (1 h). After removal of CH_3CN under reduced pressure, the resulting residue was extracted three times with CH_2Cl_2 (20 mL). The combined organic phases were washed with a 1M aqueous solution of triethylammonium acetate, dried over Na_2SO_4 and concentrated in vacuo to give a yellow solid, which was used without further purification.

The above-prepared 2-benzyl naphthoquinone derivative (200 mg, 1 equiv.) and acetic acid (5 equiv.) were added to a stirred solution of CH_3CN/H_2O (3:1, 12 mL) and heated to $85^\circ C$. $AgNO_3$ (0.35 equiv.) was added first and then $(NH_4)_2S_2O_8$ (1.3 equiv.) dissolved in 4 mL CH_3CN/H_2O (3:1) dropwise over a period of 5 min. Stirring at $85^\circ C$ was continued until TLC showed complete consumption of the starting material (3–4 h). After cooling to ambient temperature, the mixture was extracted three times with CH_2Cl_2 (20 mL). The combined organic layers were washed with H_2O , dried over Na_2SO_4 and concentrated in vacuo to give a residue, which was purified by flash chromatography as detailed below.

2-[(4-Fluorophenyl)methyl]-3-methyl-1,4-naphthoquinone (2p). Compound **2p** was purified by flash chromatography using toluene/cyclohexane (15:1). Yellow solid; yield: 17%; R_f = 0.52 (toluene:cyclohexane = 15:1); m.p.: $108\text{--}109^\circ C$ (lit [28] m.p. $114\text{--}115^\circ C$). The spectroscopic data were found to be identical to the ones described in [28]. Although **2p** represents an already known compound, to our knowledge the complete assignment of the NMR signals has not been published so far: 1H NMR (400 MHz, $DMSO-d_6$) δ = 7.26 (m, 2H, H-2', H-6'), 7.08 (t, J = 8.9 Hz, 2H, H-3', H-5'), 3.96 (s, 2H, H-9), 2.15 (s, 3H, H-10) ppm; ^{13}C NMR (100 MHz, $DMSO-d_6$) δ = 184.6 (C-4), 184.0 (C-1), 160.7 (d, $^1J_{C,F}$ = 242.0 Hz, C-4'), 144.3* (C-2), 144.2* (C-3), 134.2 (d, $^4J_{C,F}$ = 2.9 Hz, C-1'), 133.9* (C-6), 133.8* (C-7), 131.6* (C-4a), 131.4* (C-8a), 130.1 (d, $^3J_{C,F}$ = 8.0 Hz, C-2', C-6'), 125.9* (C-5), 125.8* (C-8), 115.1 (d, $^2J_{C,F}$ = 21.1 Hz, C-3', C-5'), 30.8 (C-9), 12.9 (C-10) ppm.

2-Methyl-3-[[4-(trifluoromethoxy)phenyl]methyl]-1,4-naphthoquinone (2q). Compound **2q** was purified by flash chromatography using toluene/cyclohexane (15:1). Yellow solid; yield: <5%; R_f = 0.59 (toluene:cyclohexane = 15:1); m.p.: $72\text{--}73^\circ C$ (lit [28] m.p. $65\text{--}66^\circ C$). The spectroscopic data were found to be identical to the ones described in [28]. Although

2p represents an already known compound, to our knowledge the complete assignment of the NMR signals has not been published so far: ^1H NMR (400 MHz, $\text{DMSO}-d_6$) δ = 8.01 (m, 2H, H-5, H-8), 7.84 (m, 2H, H-6, H-7), 7.36 (d, J = 8.8 Hz, 2H, H-2', H-6'), 7.25 (d, J = 8.2 Hz, 2H, H-3', H-5'), 4.01 (s, 2H, H-9), 2.16 (s, 3H, H-10) ppm; ^{13}C NMR (100 MHz, $\text{DMSO}-d_6$) δ = 184.5 (C-4), 184.0 (C-1), 146.6 (q, $^3J_{\text{C,F}}$ = 1.8 Hz, C-4'), 144.6* (C-2), 143.8* (C-3), 137.7 (C-1'), 133.9* (C-6), 133.8* (C-7), 131.7* (C-4a), 131.4* (C-8a), 130.1 (C-2', C-6'), 125.9* (C-5), 125.8* (C-8), 121.1 (C-3', C-5'), 120.0 (q, $^1J_{\text{C,F}}$ = 255.8 Hz, CF_3), 30.9 (C-9), 12.9 (C-10) ppm.

2-Methyl-3-([3-(trifluoromethoxy)phenyl]methyl)-1,4-naphthoquinone (2r). Compound **2r** was purified by flash chromatography using toluene/cyclohexane (15:1). Yellow solid; yield: <5%; R_f = 0.59 (toluene:cyclohexane = 15:1); m.p.: 70–71 °C. ^1H NMR (400 MHz, $\text{DMSO}-d_6$) δ = 8.00 (m, 2H, H-5, H-8), 7.84 (m, 2H, H-6, H-7), 7.40 (t, J = 8.1 Hz, 1H, H-5'), 7.25 (m, 2H, H-2', H-6'), 7.18 (ddt, J = 8.1, 2.4, 1.1 Hz, 1H, H-4'), 4.04 (s, 2H, H-9), 2.14 (s, 3H, H-10) ppm; ^{13}C NMR (100 MHz, $\text{DMSO}-d_6$) δ = 184.5 (C-4), 184.0 (C-1), 148.4 (q, $^3J_{\text{C,F}}$ = 1.6 Hz, C-3'), 144.8* (C-2), 143.4* (C-3), 141.0 (C-1'), 133.9* (C-6), 133.8* (C-7), 131.7* (C-4a), 131.4* (C-8a), 130.3 (C-5'), 125.9* (C-5), 125.8* (C-8), 127.3 (C-6'), 120.9 (C-2'), 120.0 (q, $^1J_{\text{C,F}}$ = 256.1 Hz, CF_3), 118.5 (C-4'), 31.3 (C-9), 12.9 (C-10) ppm; HRMS (APCI) calcd. for $\text{C}_{19}\text{H}_{13}\text{F}_3\text{O}_3$ $[\text{M}]^-$ = 346.0817; found: 346.0829.

2-([2-Fluoro-5-(trifluoromethoxy)phenyl]methyl)-3-methyl-1,4-naphthoquinone (2s). Compound **2s** was purified by flash chromatography using toluene/cyclohexane (15:1). Yellow solid; yield: <5%; R_f = 0.58 (toluene:cyclohexane = 15:1); m.p.: 78–79 °C. ^1H NMR (400 MHz, $\text{DMSO}-d_6$) δ = 8.03 (m, 1H, H-5), 7.99 (m, 1H, H-8), 7.84 (m, 2H, H-6, H-7), 7.33 (t, J = 9.1 Hz, 1H, H-3'), 7.29 (d, J = 5.4 Hz, 1H, H-6'), 7.28 (m, 1H, H-4'), 4.01 (s, 2H, H-9), 2.12 (s, 3H, H-10) ppm; ^{13}C NMR (100 MHz, $\text{DMSO}-d_6$) δ = 184.3 (C-4), 183.7 (C-1), 158.6 (d, $^1J_{\text{C,F}}$ = 244.5 Hz, C-2'), 145.6* (C-2), 144.2 (C-5'), 142.0* (C-3), 133.9* (C-6), 133.8* (C-7), 131.8 (C-4a), 131.5 (C-8a), 127.3 (d, $^2J_{\text{C,F}}$ = 18.1 Hz, C-1'), 125.9 (C-5), 125.8 (C-8), 123.2 (d, $^3J_{\text{C,F}}$ = 5.1 Hz, C-6'), 120.9 (d, $^3J_{\text{C,F}}$ = 9.1 Hz, C-4'), 119.9 (q, $^1J_{\text{C,F}}$ = 256.1 Hz, CF_3), 116.7 (d, $^2J_{\text{C,F}}$ = 24.8 Hz, C-3'), 25.3 (d, $^3J_{\text{C,F}}$ = 2.9 Hz, C-9), 12.8 (C-10) ppm; HRMS (APCI) calcd. for $\text{C}_{19}\text{H}_{12}\text{F}_4\text{O}_3$ $[\text{M}]^-$ = 364.0723; found: 364.0736.

3.1.6. General Synthetic Procedure for Benzylnaphthoquinones **4a–e** (Route B)

AgNO_3 (0.1 equiv.) and $(\text{NH}_4)_2\text{S}_2\text{O}_8$ (2 equiv.) were dissolved in water (4 mL) and a solution of 1,4-naphthoquinone (200 mg, 1 equiv.) and the respective phenylacetic acid derivative (1.4 equiv.) in a 1:1 mixture of $\text{CH}_3\text{CN}/\text{CH}_2\text{Cl}_2$ (4 mL) was quickly added. The two-phase mixture was heated to 80 °C and stirred until the TLC showed complete consumption of the starting material (1.5–2.5 h). After cooling to ambient temperature, the mixture was extracted three times with CH_2Cl_2 (20 mL). The combined organic layers were washed three times with H_2O , dried over Na_2SO_4 , and concentrated in vacuo to give a residue, which was purified by flash chromatography as detailed below.

2-Benzyl-1,4-naphthoquinone (4a). Compound **4a** was obtained after stirring for 1.5 h and purified by flash chromatography using toluene/cyclohexane (15:1). Amber solid; yield: 75%; R_f = 0.41 (toluene:cyclohexane = 15:1); m.p.: 92–93 °C (lit [70] m.p. 85–86 °C). The spectroscopic data were found to be identical to the ones described in [70]. Although **4a** represents an already known compound, to our knowledge the complete assignment of the NMR signals has not been published so far: ^1H NMR (400 MHz, CDCl_3) δ = 8.11 (m, 1H, H-8), 8.04 (m, 1H, H-5), 7.72 (m, 2H, H-6, H-7), 7.34 (m, 2H, H-3', H-5'), 7.26 (m, 1H, H-4'), 7.25 (m, 2H, H-2', H-6'), 6.61 (t, J = 1.5 Hz, 1H, H-3), 3.90 (s, 2H, H-9) ppm; ^{13}C NMR (100 MHz, CDCl_3): δ = 185.2 (C-4), 185.0 (C-1), 150.9 (C-2), 136.7 (C-1'), 135.6 (C-3), 133.8* (C-6), 133.7* (C-7), 132.2 (C-8a), 132.1 (C-4a), 129.4 (C-2', C-6'), 128.9 (C-3', C-5'), 127.0 (C-4'), 126.7 (C-8), 126.1 (C-5), 35.7 (C-9) ppm.

2-[[4-(Trifluoromethyl)phenyl]methyl]-1,4-naphthoquinone (**4b**). Compound **4b** was obtained after stirring for 2 h and purified by flash chromatography using toluene/cyclohexane (15:1). Amber solid; yield: 66%; R_f = 0.36 (toluene:cyclohexane = 15:1); m.p.: 99–100 °C (lit [26] m.p. 98–100 °C). The spectroscopic data were found to be identical to the ones described in [26]. Although **4b** represents an already known compound, to our knowledge the complete assignment of the NMR signals has not been published so far: ^1H NMR (400 MHz, DMSO- d_6) δ = 7.99 (m, 1H, H-8), 7.95 (m, 1H, H-5), 7.84 (m, 2H, H-6, H-7), 7.67 (d, J = 7.9 Hz, 2H, H-3', H-5'), 7.55 (d, J = 7.9 Hz, 2H, H-2', H-6'), 6.85 (s, 1H, H-3), 3.96 (s, 2H, H-9) ppm; ^{13}C NMR (100 MHz, DMSO- d_6): δ = 184.5 (C-4), 184.2 (C-1), 149.3 (C-2), 142.6 (C-1'), 135.8 (C-3), 134.1* (C-6), 134.0* (C-7), 131.6 (C-4a, C-8a), 129.9 (C-2', C-6'), 127.2 (q, $^2J_{\text{C,F}}$ = 31.8 Hz, C-4'), 126.1 (C-8), 125.6 (C-5), 125.3 (q, $^3J_{\text{C,F}}$ = 3.9 Hz, C-3', C-5'), 124.2 (q, $^1J_{\text{C,F}}$ = 272.1 Hz, CF₃), 34.7 (C-9) ppm.

2-[[2-Fluoro-4-(trifluoromethyl)phenyl]methyl]-1,4-naphthoquinone (**4c**). Compound **4c** was obtained after stirring for 2.5 h and purified by flash chromatography using toluene/cyclohexane (15:1). Amber solid; yield: 58%; R_f = 0.58 (toluene:cyclohexane = 15:1); m.p.: 130–131 °C. ^1H NMR (400 MHz, CDCl₃) δ = 8.12 (m, 1H, H-5), 8.05 (m, 1H, H-8), 7.75 (m, 2H, H-6, H-7), 7.45 (m, 1H, H-6'), 7.41 (m, 1H, H-5'), 7.35 (d, J = 9.7 Hz, 1H, H-3'), 6.62 (d, J = 1.6 Hz, 1H, H-3), 3.99 (s, 2H, H-9) ppm; ^{13}C NMR (100 MHz, CDCl₃): δ = 184.8 (C-4), 184.5 (C-1), 160.8 (d, $^1J_{\text{C,F}}$ = 249.2 Hz, C-2'), 148.1 (C-2), 135.8 (d, $^5J_{\text{C,F}}$ = 1.1 Hz, C-3), 134.0 (C-7), 133.9 (C-6), 132.4 (d, $^3J_{\text{C,F}}$ = 4.6 Hz, C-6'), 132.0 (C-4a, C-8a), 131.6 (qd, $^2J_{\text{C,F}}$ = 33.5, $^3J_{\text{C,F}}$ = 8.0 Hz, C-4'), 128.2 (dq, $^2J_{\text{C,F}}$ = 15.7, $^5J_{\text{C,F}}$ = 1.0 Hz, C-1'), 126.7 (C-5), 126.2 (C-8), 123.2 (qd, $^1J_{\text{C,F}}$ = 272.5, $^4J_{\text{C,F}}$ = 2.3 Hz, CF₃), 121.6 (C-5'), 113.2 (dq, $^2J_{\text{C,F}}$ = 25.1, $^3J_{\text{C,F}}$ = 3.7 Hz, C-3'), 29.2 (C-9) ppm; HRMS (ESI) calcd. for C₁₈H₉F₄O₂ [M-H][−] = 333.0544; found: 333.0550.

2-[[4-Fluoro-2-(trifluoromethyl)phenyl]methyl]-1,4-naphthoquinone (**4d**). Compound **4d** was obtained after stirring for 2.5 h and purified by flash chromatography using toluene/cyclohexane (15:1). Amber solid; yield: 61%; R_f = 0.43 (toluene:cyclohexane = 15:1); m.p.: 132–133 °C. ^1H NMR (400 MHz, CDCl₃) δ = 8.15 (m, 1H, H-5), 8.05 (m, 1H, H-8), 7.76 (m, 2H, H-6, H-7), 7.44 (dd, J = 9.0, 2.6 Hz, 1H, H-3'), 7.29 (m, 1H, H-6'), 7.25 (td, J = 8.4, 2.6 Hz, 1H, H-5'), 6.27 (s, 1H, H-3), 4.08 (s, 2H, H-9) ppm; ^{13}C NMR (100 MHz, CDCl₃): δ = 184.7 (C-4), 184.6 (C-1), 161.3 (d, $^1J_{\text{C,F}}$ = 248.7 Hz, C-4'), 150.1 (C-2), 135.8 (C-3), 134.3 (d, $^3J_{\text{C,F}}$ = 7.7 Hz, C-6'), 133.9 (C-6, C-7), 132.0 (C-4a, C-8a), 131.2 (qd, $^2J_{\text{C,F}}$ = 31.4, $^3J_{\text{C,F}}$ = 7.4 Hz, C-2'), 130.8 (C-1'), 126.8 (C-5), 126.2 (C-8), 123.3 (qd, $^1J_{\text{C,F}}$ = 274.1, $^4J_{\text{C,F}}$ = 2.7 Hz, CF₃), 119.3 (dq, $^2J_{\text{C,F}}$ = 20.7, $^5J_{\text{C,F}}$ = 1.1 Hz, C-5'), 114.3 (dq, $^2J_{\text{C,F}}$ = 25.0, $^3J_{\text{C,F}}$ = 5.7 Hz, C-3') 31.7 (C-9) ppm; HRMS (ESI) calcd. for C₁₈H₉F₄O₂ [M-H][−] = 333.0544; found: 333.0549.

2-[(6-Chloropyridin-3-yl)methyl]-1,4-naphthoquinone (**4e**). Compound **4e** was obtained after stirring for 2 h and purified by flash chromatography using toluene/cyclohexane (15:1). Amber solid; yield: 55%; R_f = 0.57 (toluene:cyclohexane = 15:1); m.p.: 154–155 °C. ^1H NMR (400 MHz, CDCl₃) δ = 8.34 (d, J = 2.5 Hz, 1H, H-2'), 8.09 (dd, J = 5.8, 3.4 Hz, 1H, H-8), 8.06 (dd, J = 5.7, 3.4 Hz, 1H, H-5), 7.75 (m, 2H, H-6, H-7), 7.58 (dd, J = 8.2, 2.5 Hz, 1H, H-4'), 7.30 (d, 8.2 Hz, 1H, H-5'), 6.68 (s, 1H, H-3), 3.88 (s, 2H, H-9) ppm; ^{13}C NMR (100 MHz, CDCl₃): δ = 184.7 (C-4), 184.6 (C-1), 150.3 (C-2', C-6'), 149.0 (C-2), 139.7 (C-4'), 135.9 (C-3), 134.1* (C-6), 134.0* (C-7), 132.0* (C-4a), 131.9* (C-8a), 131.6 (C-3'), 126.8 (C-8), 126.3 (C-5), 124.4 (C-5'), 32.6 (C-9) ppm; HRMS (APCI) calcd. for C₁₆H₁₁ClNO₂ [M+H]⁺ = 284.0473; found: 284.0465.

3.1.7. General Synthetic Procedure for Trifluoromenadiones **5a–c** (Route B)

CuI (0.5 equiv.), bis(pinacolato)diboron (B₂pin₂, 0.01 equiv.), and Togni reagent (2 equiv.) were dissolved in CHCl₃ (3 mL) in the strict exclusion of air or moisture, and the mixture was refluxed in an oil bath at 85 °C. The corresponding benzylnaphthoquinone

derivative (200 mg, 1 equiv.) dissolved in 5 mL of CHCl_3 was then added, and stirring was continued at 85 °C until TLC showed complete consumption of the starting material (20–26 h). After cooling to ambient temperature, the mixture was diluted with CHCl_3 (20 mL) and washed with H_2O (15 mL) three times. The organic layer was dried over Na_2SO_4 and then concentrated in vacuo to give a residue, which was purified by flash chromatography as detailed below.

2-Benzyl-3-(trifluoromethyl)-1,4-naphthoquinone (5a). Compound **5a** was obtained from **4a** after stirring for 20 h and purified by flash chromatography using toluene/cyclohexane (15:1). Yellow solid; yield: 60%; R_f = 0.49 (toluene:cyclohexane = 15:1); m.p.: 72–73 °C. ^1H NMR (400 MHz, $\text{DMSO}-d_6$) δ = 8.06 (m, 1H, H-5), 8.03 (m, 1H, H-8), 7.93 (m, 1H, H-6), 7.89 (m, 1H, H-7), 7.28 (m, 2H, H-3', H-5'), 7.20 (dd, J = 7.5, 1.8 Hz, 2H, H-2', H-6'), 7.18 (m, 1H, H-4'), 4.18 (s, 2H, H-9) ppm; ^{13}C NMR (100 MHz, $\text{DMSO}-d_6$): δ = 183.3 (C-1), 180.3 (C-4), 149.2 (q, $^3J_{\text{C,F}}$ = 1.8 Hz, C-2), 137.5 (C-1'), 134.7 (C-6), 134.4 (C-7), 132.4 (q, $^2J_{\text{C,F}}$ = 27.0 Hz, C-3), 131.6 (q, $^4J_{\text{C,F}}$ = 1.5 Hz, C-4a), 131.0 (C-8a), 128.4 (C-3', C-5'), 127.9 (C-2', C-6'), 126.4 (C-8), 126.2 (C-4'), 125.9 (C-5), 122.4 (q, $^1J_{\text{C,F}}$ = 278.1 Hz, C-10), 31.7 (q, $^4J_{\text{C,F}}$ = 3.3 Hz, C-9) ppm; HRMS (APCI) calcd. for $\text{C}_{18}\text{H}_{11}\text{F}_3\text{O}_2$ $[\text{M}]^-$ = 316.0711; found: 316.0719.

2-(Trifluoromethyl)-3-([4-(trifluoromethyl)phenyl]methyl)-1,4-naphthoquinone (5b). Compound **5b** was obtained from **4b** after stirring for 24 h and purified by flash chromatography using toluene/cyclohexane (15:1). Yellow solid; yield: 57%; R_f = 0.32 (toluene:cyclohexane = 15:1); m.p.: 83–84 °C. ^1H NMR (400 MHz, $\text{DMSO}-d_6$) δ = 8.07 (m, 1H, H-5), 8.03 (m, 1H, H-8), 7.94 (td, J = 7.4, 1.7 Hz, 1H, H-6), 7.90 (td, J = 7.4, 1.6 Hz, 1H, H-7), 7.63 (d, J = 8.2 Hz, 2H, H-3', H-5'), 7.46 (d, J = 8.2 Hz, 2H, H-2', H-6'), 4.26 (s, 2H, H-9) ppm; ^{13}C NMR (100 MHz, $\text{DMSO}-d_6$): δ = 183.2 (C-1), 180.2 (C-4), 148.4 (q, $^3J_{\text{C,F}}$ = 1.8 Hz, C-2), 142.6 (C-1'), 134.7 (C-6), 134.4 (C-7), 132.9 (q, $^2J_{\text{C,F}}$ = 27.1 Hz, C-3), 131.7 (q, $^4J_{\text{C,F}}$ = 1.5 Hz, C-4a), 131.1 (C-8a), 128.8 (C-2', C-6'), 127.0 (q, $^2J_{\text{C,F}}$ = 31.9 Hz, C-4'), 126.4 (C-8), 125.9 (C-5), 125.2 (q, $^3J_{\text{C,F}}$ = 3.9 Hz, C-3', C-5'), 124.2 (q, $^1J_{\text{C,F}}$ = 278.1 Hz, 4'-CF₃), 122.3 (q, $^1J_{\text{C,F}}$ = 278.3 Hz, C-10), 31.7 (q, $^4J_{\text{C,F}}$ = 3.2 Hz, C-9) ppm; HRMS (APCI) calcd. for $\text{C}_{19}\text{H}_{10}\text{F}_6\text{O}_2$ $[\text{M}]^-$ = 384.0585; found: 384.0584.

2-([2-Fluoro-4-(trifluoromethyl)phenyl]methyl)-3-(trifluoromethyl)-1,4-naphthoquinone (5c). Compound **5c** was obtained from **4c** after stirring for 26 h and purified by flash chromatography using toluene/cyclohexane (15:1). Yellow solid; yield: 40%; R_f = 0.30 (toluene:cyclohexane = 15:1); m.p.: 75–76 °C. ^1H NMR (400 MHz, $\text{DMSO}-d_6$) δ = 8.09 (m, 1H, H-5), 8.04 (m, 1H, H-8), 7.95 (td, J = 7.5, 1.7 Hz, 1H, H-6), 7.92 (td, J = 7.4, 1.6 Hz, 1H, H-7), 7.69 (m, 1H, H-3'), 7.47 (m, 2H, H-5', H-6'), 4.21 (s, 2H, H-9) ppm; ^{13}C NMR (100 MHz, $\text{DMSO}-d_6$): δ = 182.9 (C-1), 180.1 (C-4), 159.5 (d, $^1J_{\text{C,F}}$ = 247.4 Hz, C-2'), 147.6 (q, $^3J_{\text{C,F}}$ = 2.8 Hz, C-2), 134.8 (C-6), 134.5 (C-7), 133.3 (q, $^2J_{\text{C,F}}$ = 27.2 Hz, C-3), 131.6 (C-4a), 131.1 (C-8a), 130.8 (qd, $^2J_{\text{C,F}}$ = 33.2, $^3J_{\text{C,F}}$ = 8.0 Hz, C-4', C-6'), 129.6 (d, $^2J_{\text{C,F}}$ = 32.2 Hz, C-1'), 126.4 (C-8), 126.0 (C-5), 123.3 (qd, $^1J_{\text{C,F}}$ = 272.0, $^4J_{\text{C,F}}$ = 2.5 Hz, 4'-CF₃), 122.3 (q, $^1J_{\text{C,F}}$ = 278.1 Hz, C-10), 121.4 (C-5'), 112.6 (dq, $^2J_{\text{C,F}}$ = 25.6, $^3J_{\text{C,F}}$ = 3.8 Hz, C-3'), 25.4 (dq, $^3J_{\text{C,F}}$ = 6.1, $^4J_{\text{C,F}}$ = 3.1 Hz, C-9) ppm; HRMS (APCI) calcd. for $\text{C}_{19}\text{H}_9\text{F}_7\text{O}_2$ $[\text{M}]^-$ = 402.0498; found: 402.0501.

4. Conclusions

In this study, we present the synthesis of 27 plasmodione-like benzylnaphthoquinone derivatives together with their antiprotozoal activities and physicochemical parameters. The antiplasmodial potential was found highly promising, which was also confirmed by remarkably high selectivities. Ligand efficiency metrics, specifically size-independent ligand efficiency (SILE), correlated strongly with antiplasmodial activity, thus guiding drug optimization.

The four-fold fluorinated benzylmenadione **2e** showed the lowest IC₅₀ of all prepared compounds against the *P. falciparum* NF54 strain at 0.006 µM along with very good selectivity (SI = 7495). The trypanocidal effect among the synthesized compounds was also assessed. It was found strongest in benzyl-NQ, **4a**, albeit much less pronounced.

The findings presented in this work demonstrate the potential of benzylmenadiones as promising chemical leads in the development of new antiplasmodial drugs.

Supplementary Materials: The following supporting information can be downloaded at: <https://www.mdpi.com/article/10.3390/ijms26052114/s1>.

Author Contributions: Conceptualization, A.P.; methodology, A.P.; software, A.P.; validation, A.P. and W.S.; formal analysis, A.P.; investigation, A.P., G.B., E.-M.P.-W., M.K. and P.M.; resources, A.P., E.-M.P.-W., M.K. and P.M.; data curation, A.P., E.-M.P.-W., M.K., P.M. and W.S.; writing—original draft preparation, A.P. and W.S.; writing—review and editing, A.P., E.-M.P.-W., M.K., P.M. and W.S.; visualization, A.P.; supervision, A.P.; project administration, A.P.; funding acquisition, A.P. All authors have read and agreed to the published version of the manuscript.

Funding: This research received no external funding.

Institutional Review Board Statement: Not applicable.

Informed Consent Statement: Not applicable.

Data Availability Statement: The data presented in this study are available on request from corresponding author.

Acknowledgments: The authors are grateful to R. Weis for discussions and to the University of Graz for Open Access Funding. NAWI Graz is acknowledged for supporting the Graz Central Lab Environmental, Plant, and Microbial Metabolomics.

Conflicts of Interest: The authors declare no conflicts of interest.

References

1. WHO Global Malaria Programme. World Malaria Report 2023. World Health Organization [Online]. 30 November 2023. Available online: <https://www.who.int/publications/i/item/9789240086173> (accessed on 8 October 2024).
2. WHO Global Malaria Programme. Global Technical Strategy for Malaria 2016–2030, 2021 Update. World Health Organization [Online]. 19 July 2021. Available online: <https://www.who.int/publications/i/item/9789240031357> (accessed on 8 October 2024).
3. Parums, D.V. Editorial: Current Status of Two Adjuvanted Malaria Vaccines and the World Health Organization (WHO) Strategy to Eradicate Malaria by 2030. *Med. Sci. Monit.* **2023**, *29*, e939357. [CrossRef]
4. Poespoprodjo, J.R.; Douglas, N.M.; Ansong, D.; Kho, S.; Anstey, N.M. Malaria. *Lancet* **2023**, *402*, 2328–2345. [CrossRef] [PubMed]
5. Pérez-Pertejo, Y.; Escudero-Martínez, J.M.; Reguera, R.M.; Balaña-Fouce, R.; García, P.A.; Jambrina, P.G.; San Feliciano, A.; Castro, M.-Á. Antileishmanial activity of terpenylquinones on *Leishmania infantum* and their effects on *Leishmania* topoisomerase IB. *Int. J. Parasitol. Drugs Drug Resist.* **2019**, *11*, 70–79. [CrossRef]
6. Jentzsch, J.; Koko, W.S.; Al Nasr, I.S.; Khan, T.A.; Schobert, R.; Ersfeld, K.; Biersack, B. New Antiparasitic Bis-Naphthoquinone Derivatives. *Chem. Biodivers.* **2020**, *17*, e1900597. [CrossRef] [PubMed]
7. Rivera, G.; Patel, N.B.; Bandyopadhyay, D. Editorial: Discovery and Development of Drugs for Neglected Diseases: Chagas Disease, Human African Trypanosomiasis, and Leishmaniasis. *Front. Chem.* **2021**, *9*, 775327. [CrossRef]
8. Prieto Cardenas, L.S.; Arias Soler, K.A.; Nossa Gonzalez, D.L.; Roza Nunez, W.E.; Cardenas-Chaparro, A.; Duchowicz, P.R.; Gomez Castano, J.A. In Silico Antiprotozoal Evaluation of 1,4-Naphthoquinone Derivatives against Chagas and Leishmaniasis Diseases Using QSAR, Molecular Docking, and ADME Approaches. *Pharmaceuticals* **2022**, *15*, 687. [CrossRef] [PubMed]
9. Fotie, J. Quinones and malaria. *Anti-Infect. Agents Med. Chem.* **2006**, *5*, 357–366. [CrossRef]
10. Ventura Pinto, A.; Lisboa de Castro, S. The trypanocidal activity of naphthoquinones: A review. *Molecules* **2009**, *14*, 4570–4590. [CrossRef] [PubMed]
11. Andujar, I.; Rios, J.L.; Giner, R.M.; Recio, M.C. Pharmacological properties of shikonin—A review of literature since 2002. *Planta Med.* **2013**, *79*, 1685–1697. [CrossRef] [PubMed]
12. Futuro, D.O.; Ferreira, V.F.; Ferreira, P.G.; Nicoletti, C.D.; Borba-Santos, L.P.; Rozental, S.; Silva, F.C.D. The Antifungal Activity of Naphthoquinones: An Integrative Review. *An. Acad. Bras. Cienc.* **2018**, *90*, 1187–1214. [CrossRef]

13. Patel, O.P.S.; Beteck, R.M.; Legoabe, L.J. Antimalarial application of quinones: A recent update. *Eur. J. Med. Chem.* **2021**, *210*, 113084. [\[CrossRef\]](#)
14. Pérez-Sacau, E.; Estévez-Braun, A.; Ravelo, A.G.; Gutiérrez Yapu, D.; Giménez Turba, A. Antiplasmodial activity of naphthoquinones related to lapachol and β -lapachone. *Chem. Biodivers.* **2005**, *2*, 264–274. [\[CrossRef\]](#)
15. Grellier, P.; Marozienne, A.; Nivinskas, H.; Sarlauskas, J.; Aliverti, A.; Cenas, N. Antiplasmodial activity of quinones: Roles of aziridinyl substituents and the inhibition of *Plasmodium falciparum* glutathione reductase. *Arch. Biochem. Biophys.* **2010**, *494*, 32–39. [\[CrossRef\]](#) [\[PubMed\]](#)
16. Hughes, L.M.; Lanteri, C.A.; O’Neil, M.T.; Johnson, J.D.; Gribble, G.W.; Trumpower, B.L. Design of antiparasitic and antifungal hydroxy-naphthoquinones that are less susceptible to drug resistance. *Mol. Biochem. Parasitol.* **2011**, *177*, 12–19. [\[CrossRef\]](#) [\[PubMed\]](#)
17. Sumsakul, W.; Plengsuriyakarn, T.; Chaijaroenkul, W.; Viyanant, V.; Karbwang, J.; Na-Bangchang, K. Antimalarial activity of plumbagin in vitro and in animal models. *BMC Complement. Altern. Med.* **2014**, *14*, 15. [\[CrossRef\]](#)
18. Muller, T.; Johann, L.; Jannack, B.; Bruckner, M.; Lanfranchi, D.A.; Bauer, H.; Sanchez, C.; Yardley, V.; Deregnacourt, C.; Schrevel, J.; et al. Glutathione Reductase-Catalyzed Cascade of Redox Reactions to Bioactivate Potent Antimalarial 1,4-Naphthoquinones—A New Strategy to Combat Malarial Parasites. *J. Am. Chem. Soc.* **2011**, *133*, 11557–11571. [\[CrossRef\]](#)
19. Bielitz, M.; Belorgey, D.; Ehrhardt, K.; Johann, L.; Lanfranchi, D.A.; Gallo, V.; Schwarzer, E.; Mohring, F.; Jortzik, E.; Williams, D.L.; et al. Antimalarial NADPH-Consuming Redox-Cyclers As Superior Glucose-6-Phosphate Dehydrogenase Deficiency Copycats. *Antioxid. Redox Signal.* **2015**, *22*, 1337–1351. [\[CrossRef\]](#)
20. Sidorov, P.; Desta, I.; Chesse, M.; Horvath, D.; Marcou, G.; Varnek, A.; Davioud-Charvet, E.; Elhabiri, M. Redox Polypharmacology as an Emerging Strategy to Combat Malarial Parasites. *ChemMedChem* **2016**, *11*, 1339–1351. [\[CrossRef\]](#) [\[PubMed\]](#)
21. Ehrhardt, K.; Deregnacourt, C.; Goetz, A.-A.; Tzanova, T.; Gallo, V.; Arese, P.; Pradines, B.; Adjalley, S.H.; Bagrel, D.; Blandin, S.; et al. The redox cyclers plasmodione is a fast-acting antimalarial lead compound with pronounced activity against sexual and early asexual blood-stage parasites. *Antimicrob. Agents Chemother.* **2016**, *60*, 5146–5158. [\[CrossRef\]](#)
22. Iacobucci, I.; Monaco, V.; Hovasse, A.; Dupouy, B.; Keumoe, R.; Cichocki, B.; Elhabiri, M.; Meunier, B.; Strub, J.-M.; Monti, M.; et al. Proteomic Profiling of Antimalarial Plasmodione Using 3-Benz(o)ylmenadione Affinity-Based Probes. *ChemBioChem* **2024**, *25*, e202400187. [\[CrossRef\]](#) [\[PubMed\]](#)
23. Mounkoro, P.; Michel, T.; Golinelli-Cohen, M.-P.; Blandin, S.; Davioud-Charvet, E.; Meunier, B. A role for the succinate dehydrogenase in the mode of action of the redox-active antimalarial drug, plasmodione. *Free Radic. Biol. Med.* **2021**, *162*, 533–541. [\[CrossRef\]](#)
24. Kumar Jha, R.; Kumar, S. Direct Functionalization of *para*-Quinones: A Historical Review and New Perspectives. *Eur. J. Org. Chem.* **2024**, *27*, e202400535. [\[CrossRef\]](#)
25. Donzel, M.; Karabiyikli, D.; Cotos, L.; Elhabiri, M.; Davioud-Charvet, E. Direct C-H Radical Alkylation of 1,4-Quinones. *Eur. J. Org. Chem.* **2021**, *2021*, 3622–3633. [\[CrossRef\]](#)
26. Rodo, E.C.; Feng, L.; Jida, M.; Ehrhardt, K.; Bielitz, M.; Boilevin, J.; Lanzer, M.; Williams, D.L.; Lanfranchi, D.A.; Davioud-Charvet, E. A Platform of Regioselective Methodologies to Access Polysubstituted 2-Methyl-1,4-naphthoquinone Derivatives: Scope and Limitations. *Eur. J. Org. Chem.* **2016**, *2016*, 1982–1993. [\[CrossRef\]](#)
27. Li, D.; Shen, X. Iron-catalyzed regioselective alkylation of 1,4-quinones and coumarins with functionalized alkyl bromides. *Org. Biomol. Chem.* **2020**, *18*, 750–754. [\[CrossRef\]](#)
28. Donzel, M.; Elhabiri, M.; Davioud-Charvet, E. Bioinspired Photoredox Benzoylation of Quinones. *J. Org. Chem.* **2021**, *86*, 10055–10066. [\[CrossRef\]](#) [\[PubMed\]](#)
29. Feng, L.; Lanfranchi, D.A.; Cotos, L.; Cesar-Rodo, E.; Ehrhardt, K.; Goetz, A.-A.; Zimmermann, H.; Fenaille, F.; Blandin, S.A.; Davioud-Charvet, E. Synthesis of plasmodione metabolites and ^{13}C -enriched plasmodione as chemical tools for drug metabolism investigation. *Org. Biomol. Chem.* **2018**, *16*, 2647–2665. [\[CrossRef\]](#)
30. Anderson, J.M.; Kochi, J.K. Silver(I)-catalyzed oxidative decarboxylation of acids by peroxydisulfate. Role of silver(II). *J. Am. Chem. Soc.* **1970**, *92*, 1651. [\[CrossRef\]](#)
31. Lanfranchi, D.A.; Belorgey, D.; Mueller, T.; Vezin, H.; Lanzer, M.; Davioud-Charvet, E. Exploring the trifluoromenadione core as a template to design antimalarial redox-active agents interacting with glutathione reductase. *Org. Biomol. Chem.* **2012**, *10*, 4795–4806. [\[CrossRef\]](#) [\[PubMed\]](#)
32. Ilchenko, N.O.; Janson, P.G.; Szabo, K.J. Copper-mediated C-H trifluoromethylation of quinones. *Chem. Commun.* **2013**, *49*, 6614–6616. [\[CrossRef\]](#) [\[PubMed\]](#)
33. Wang, X.; Ye, Y.; Ji, G.; Xu, Y.; Zhang, S.; Feng, J.; Zhang, Y.; Wang, J. Copper-Catalyzed Direct C-H Trifluoromethylation of Quinones. *Org. Lett.* **2013**, *15*, 3730–3733. [\[CrossRef\]](#)
34. Fang, Z.; Ning, Y.; Mi, P.; Liao, P.; Bi, X. Catalytic C-H α -Trifluoromethylation of α,β -Unsaturated Carbonyl Compounds. *Org. Lett.* **2014**, *16*, 1522–1525. [\[CrossRef\]](#)

35. Urgin, K.; Jida, M.; Ehrhardt, K.; Muller, T.; Lanzer, M.; Maes, L.; Elhabiri, M.; Davioud-Charvet, E. Pharmacomodulation of the antimalarial plasmodione: Synthesis of biaryl- and *N*-arylalkylamine analogues, antimalarial activities and physicochemical properties. *Molecules* **2017**, *22*, 161. [\[CrossRef\]](#)
36. Nwaka, S.; Ramirez, B.; Brun, R.; Maes, L.; Douglas, F.; Ridley, R. Advancing drug innovation for neglected diseases-criteria for lead progression. *PLoS Negl. Trop. Dis.* **2009**, *3*, e440. [\[CrossRef\]](#)
37. Katsuno, K.; Burrows, J.n.; Duncan, K.; van Huijsduijnen, R.H.; Kaneko, T.; Kita, K.; Mowbray, C.E.; Schmatz, D.; Warner, P.; Slingsby, B.T. Hit and lead criteria in drug discovery for infectious diseases of the developing world. *Nat. Rev. Drug Discov.* **2015**, *14*, 751–758. [\[CrossRef\]](#) [\[PubMed\]](#)
38. Samby, K.; Willis, P.a.; Burrows, J.n.; Laleu, B.; Webborn, P.j.h. Actives from MMV Open Access Boxes? A suggested way forward. *PLoS Pathog.* **2021**, *17*, e1009384. [\[CrossRef\]](#) [\[PubMed\]](#)
39. Banerjee, P.; Kemmler, E.; Dunkel, M.; Preissner, R. ProTox 3.0: A webserver for the prediction of toxicity of chemicals. *Nucleic Acids Res.* **2024**, *52*, W513–W520. [\[CrossRef\]](#)
40. de Sena Pereira, V.S.; de Oliveira, C.B.S.; Fumagalli, F.; da Silva Emery, F.; da Silva, N.B.; de Andrade-Neto, V.F. Cytotoxicity, hemolysis and in vivo acute toxicity of 2-hydroxy-3-anilino-1,4-naphthoquinone derivatives. *Toxicol. Rep.* **2016**, *3*, 756–762. [\[CrossRef\]](#) [\[PubMed\]](#)
41. Gleeson, M.P.; Hersey, A.; Montanari, D.; Overington, J. Probing the links between in vitro potency, ADMET and physicochemical parameters. *Nat. Rev. Drug Discov.* **2011**, *10*, 197–208. [\[CrossRef\]](#) [\[PubMed\]](#)
42. Meanwell, N.A. Improving Drug Candidates by Design: A Focus on Physicochemical Properties As a Means of Improving Compound Disposition and Safety. *Chem. Res. Toxicol.* **2011**, *24*, 1420–1456. [\[CrossRef\]](#) [\[PubMed\]](#)
43. Tinworth, C.P.; Young, R.J. Facts, Patterns, and Principles in Drug Discovery: Appraising the Rule of 5 with Measured Physicochemical Data. *J. Med. Chem.* **2020**, *63*, 10091–10108. [\[CrossRef\]](#) [\[PubMed\]](#)
44. Lipinski, C.A.; Lombardo, F.; Dominy, B.W.; Feeney, P.J. Experimental and computational approaches to estimate solubility and permeability in drug discovery and development settings. *Adv. Drug Deliv. Rev.* **1997**, *23*, 3–25. [\[CrossRef\]](#)
45. Lipinski, C.A.; Lombardo, F.; Dominy, B.W.; Feeney, P.J. Experimental and computational approaches to estimate solubility and permeability in drug discovery and development settings. *Adv. Drug Deliv. Rev.* **2001**, *46*, 3–26. [\[CrossRef\]](#)
46. Veber, D.F.; Johnson, S.R.; Cheng, H.-Y.; Smith, B.R.; Ward, K.W.; Kopple, K.D. Molecular Properties That Influence the Oral Bioavailability of Drug Candidates. *J. Med. Chem.* **2002**, *45*, 2615–2623. [\[CrossRef\]](#) [\[PubMed\]](#)
47. Hann, M.M. Molecular obesity, potency and other addictions in drug discovery. *MedChemComm* **2011**, *2*, 349–355. [\[CrossRef\]](#)
48. Tarcsay, A.; Keseru, G.M. Contributions of Molecular Properties to Drug Promiscuity. *J. Med. Chem.* **2013**, *56*, 1789–1795. [\[CrossRef\]](#)
49. Mignani, S.; Rodrigues, J.; Tomas, H.; Jalal, R.; Singh, P.P.; Majoral, J.-P.; Vishwakarma, R.A. Present drug-likeness filters in medicinal chemistry during the hit and lead optimization process: How far can they be simplified? *Drug Discov. Today* **2018**, *23*, 605–615. [\[CrossRef\]](#) [\[PubMed\]](#)
50. Young, R.J.; Flitsch, S.L.; Grigalunas, M.; Leeson, P.D.; Quinn, R.J.; Turner, N.J.; Waldmann, H. The Time and Place for Nature in Drug Discovery. *JACS Au* **2022**, *2*, 2400–2416. [\[CrossRef\]](#) [\[PubMed\]](#)
51. Hopkins, A.L.; Keseru, G.M.; Leeson, P.D.; Rees, D.C.; Reynolds, C.H. The role of ligand efficiency metrics in drug discovery. *Nat. Rev. Drug Discov.* **2014**, *13*, 105–121. [\[CrossRef\]](#)
52. Johnson, T.W.; Gallego, R.A.; Edwards, M.P. Lipophilic efficiency as an important metric in drug design. *J. Med. Chem.* **2018**, *61*, 6401–6420. [\[CrossRef\]](#)
53. Scott, J.S.; Waring, M.J. Practical application of ligand efficiency metrics in lead optimisation. *Bioorg. Med. Chem.* **2018**, *26*, 3006–3015. [\[CrossRef\]](#)
54. Leeson, P.D.; Bento, A.P.; Gaulton, A.; Hersey, A.; Mannes, E.J.; Radoux, C.J.; Leach, A.R. Target-Based Evaluation of “Drug-Like” Properties and Ligand Efficiencies. *J. Med. Chem.* **2021**, *64*, 7210–7230. [\[CrossRef\]](#) [\[PubMed\]](#)
55. Abad-Zapatero, C. Ligand efficiency indices for effective drug discovery: A unifying vector formulation. *Expert. Opin. Drug Discov.* **2021**, *16*, 763–775. [\[CrossRef\]](#) [\[PubMed\]](#)
56. Nissink, J.W.M. Simple Size-Independent Measure of Ligand Efficiency. *J. Chem. Inf. Model.* **2009**, *49*, 1617–1622. [\[CrossRef\]](#) [\[PubMed\]](#)
57. Cavalluzzi, M.M.; Mangiatordi, G.F.; Nicolotti, O.; Lentini, G. Ligand efficiency metrics in drug discovery: The pros and cons from a practical perspective. *Expert. Opin. Drug Discov.* **2017**, *12*, 1087–1104. [\[CrossRef\]](#) [\[PubMed\]](#)
58. Doak, B.C.; Over, B.; Giordanetto, F.; Kihlberg, J. Oral Druggable Space beyond the Rule of 5: Insights from Drugs and Clinical Candidates. *Chem. Biol.* **2014**, *21*, 1115–1142. [\[CrossRef\]](#)
59. Price, E.; Weinheimer, M.; Rivkin, A.; Jenkins, G.; Nijsen, M.; Cox, P.B.; DeGoey, D. Beyond Rule of Five and PROTACs in Modern Drug Discovery: Polarity Reducers, Chameleonicity, and the Evolving Physicochemical Landscape. *J. Med. Chem.* **2024**, *67*, 5683–5698. [\[CrossRef\]](#)

60. DeGoey, D.A.; Chen, H.-J.; Cox, P.B.; Wendt, M.D. Beyond the Rule of 5: Lessons Learned from AbbVie's Drugs and Compound Collection. *J. Med. Chem.* **2018**, *61*, 2636–2651. [[CrossRef](#)] [[PubMed](#)]
61. Young, R.J.; Green, D.V.S.; Luscombe, C.N.; Hill, A.P. Getting physical in drug discovery II: The impact of chromatographic hydrophobicity measurements and aromaticity. *Drug Discov. Today* **2011**, *16*, 822–830. [[CrossRef](#)]
62. Wager, T.T.; Hou, X.; Verhoest, P.R.; Villalobos, A. Central Nervous System Multiparameter Optimization Desirability: Application in Drug Discovery. *ACS Chem. Neurosci.* **2016**, *7*, 767–775. [[CrossRef](#)] [[PubMed](#)]
63. Wager, T.T.; Hou, X.; Verhoest, P.R.; Villalobos, A. Moving beyond Rules: The Development of a Central Nervous System Multiparameter Optimization (CNS MPO) Approach to Enable Alignment of Druglike Properties. *ACS Chem. Neurosci.* **2010**, *1*, 435–449. [[CrossRef](#)]
64. Bickerton, G.R.; Paolini, G.V.; Besnard, J.; Muresan, S.; Hopkins, A.L. Quantifying the chemical beauty of drugs. *Nat. Chem.* **2012**, *4*, 90–98. [[CrossRef](#)] [[PubMed](#)]
65. Sun, L.; Zhang, M.; Xie, L.; Xu, X.; Xu, P.; Xu, L. Computational prediction of Lee retention indices of polycyclic aromatic hydrocarbons by using machine learning. *Chem. Biol. Drug Des.* **2023**, *101*, 380–394. [[CrossRef](#)] [[PubMed](#)]
66. Mortenson, P.N.; Murray, C.W. Assessing the lipophilicity of fragments and early hits. *J. Comput.-Aided Mol. Des.* **2011**, *25*, 663–667. [[CrossRef](#)]
67. Young, R.J.; Leeson, P.D. Mapping the Efficiency and Physicochemical Trajectories of Successful Optimizations. *J. Med. Chem.* **2018**, *61*, 6421–6467. [[CrossRef](#)] [[PubMed](#)]
68. Abad-Zapatero, C.; Blasi, D. Ligand Efficiency Indices (LEIs): More than a Simple Efficiency Yardstick. *Mol. Inform.* **2011**, *30*, 122–132. [[CrossRef](#)] [[PubMed](#)]
69. Abad-Zapatero, C.; Perisic, O.; Wass, J.; Bento, A.P.; Overington, J.; Al-Lazikani, B.; Johnson, M.E. Ligand efficiency indices for an effective mapping of chemico-biological space: The concept of an atlas-like representation. *Drug Discov. Today* **2010**, *15*, 804–811. [[CrossRef](#)]
70. Skrzynska, A.; Romaniszyn, M.; Pomiklo, D.; Albrecht, L. The Application of 2-Benzyl-1,4-naphthoquinones as Pronucleophiles in Aminocatalytic Synthesis of Tricyclic Derivatives. *J. Org. Chem.* **2018**, *83*, 5019–5026. [[CrossRef](#)] [[PubMed](#)]

Disclaimer/Publisher's Note: The statements, opinions and data contained in all publications are solely those of the individual author(s) and contributor(s) and not of MDPI and/or the editor(s). MDPI and/or the editor(s) disclaim responsibility for any injury to people or property resulting from any ideas, methods, instructions or products referred to in the content.